

1 **Quantifying the $\delta^{15}\text{N}$ trophic offset in a cold-water scleractinian coral**
2 **(CWC): implications for the CWC diet and coral $\delta^{15}\text{N}$ as the marine N**
3 **cycle proxy.**

4 Josie L. Mottram¹, Anne M. Gothmann², Maria G. Prokopenko³, Austin Cordova³, Veronica Rollinson¹,
5 Katie Dobkowski⁴, Julie Granger¹

6 ¹Department of Marine Sciences, University of Connecticut, Storrs, CT, 06340, USA

7 ²Departments of Physics and Environmental Studies, St. Olaf College, Northfield, MN, 55057, USA

8 ³Department of Geology, Pomona College, Claremont, CA, 91711, USA

9 ⁴Department of Environmental Studies, Woodbury University, Burbank, CA, 91504, USA

10 Correspondence to: Anne M. Gothmann (gothma1@stolaf.edu)

11 **Abstract.** The nitrogen (N) isotope composition ($\delta^{15}\text{N}$) of cold-water corals is a promising proxy for
12 reconstructing past ocean N cycling, as a strong correlation was found between the $\delta^{15}\text{N}$ of the organic
13 nitrogen preserved in coral skeletons and the $\delta^{15}\text{N}$ of particulate organic matter exported from the
14 surface ocean. However, a large offset of 8-9 ‰ between the $\delta^{15}\text{N}$ recorded by the coral and that of
15 exported particulate organic matter remains unexplained. The 8-9 ‰ offset may signal a higher trophic
16 level of coral dietary sources, an unusually large trophic isotope effect or a biosynthetic $\delta^{15}\text{N}$ offset
17 between the coral's soft tissue and skeletal organic matter, or some combinations of these factors. To
18 understand the origin of the offset and further validate the proxy, we investigated the trophic ecology of
19 the asymbiotic scleractinian cold water coral *Balanophyllia elegans*, both in a laboratory setting and in
20 its natural habitat. A long-term incubation experiment of *B. elegans* fed on an isotopically controlled
21 diet yielded a canonical trophic isotope effect of 3.0 ± 0.1 ‰ between coral soft tissue and the *Artemia*
22 prey. The trophic isotope effect was not detectably influenced by sustained food limitation. A long N
23 turnover of coral soft tissue, expressed as an e-folding time, of 291 ± 15 days in the well-fed
24 incubations indicates that coral skeleton $\delta^{15}\text{N}$ is not likely to track subannual (e.g. seasonal) variability
25 of diet $\delta^{15}\text{N}$. Specimens of *B. elegans* from the subtidal zone near San Juan Channel (WA, USA)
26 revealed a modest difference between soft tissue and skeletal $\delta^{15}\text{N}$ of 1.2 ± 0.6 ‰. The $\delta^{15}\text{N}$ of the coral
27 soft tissue was 12.0 ± 0.6 ‰, which was ~6 ‰ higher than that of suspended organic material that was
28 comprised dominantly of phytoplankton – suggesting that phytoplankton is not the primary component
29 of *B. elegans*' diet. An analysis of size-fractionated net tow material suggests that *B. elegans* fed
30 predominantly on a size class of zooplankton ≥ 500 μm , implicating a two-level trophic transfer
31 between phytoplankton material and coral tissue. These results point to a feeding strategy that may
32 result in an influence of regional food web structure on the cold-water coral $\delta^{15}\text{N}$. This factor should be
33 taken into consideration when applying the proxy to paleoceanographic studies of ocean N cycling.

Formatted ... [1]

Deleted:

Deleted:

Deleted: the

Formatted ... [2]

Deleted: Zooplankton as the primary diet for cold-water scleractinian corals (CWCs): implications for the CWC marine N cycle proxy and trophic ecology.

Formatted: Font: 16 pt

Formatted: Font color: Text 1

Formatted ... [3]

Deleted: sinking ...articulate organic matter exported from the surface ocean. However, a large offset of 8-9 ‰ between the $\delta^{15}\text{N}$ recorded by the coral and that of exported particulate organic matter remains unexplained. The 8-9 ‰ offset may signal a higher trophic level of coral dietary sources, potential sensitivity of the proxy to food web structure, ...n unusually large trophic isotope effect or a biosynthetic $\delta^{15}\text{N}$ offset between the coral's soft tissue and skeletal tissues

Formatted ... [4]

Formatted ... [5]

Deleted: the

Deleted: .

Deleted: the ...oral skeleton is not apt

Deleted: is not able to provide sufficient resolution to

Deleted:

Deleted: ity

Formatted ... [7]

Deleted: to record seasonal difference in

Deleted: shallow

Deleted: tissue ...¹⁵N of 1.2 ± 0.6 ‰. The $\delta^{15}\text{N}$ of the coral soft tissue was 12.0 ± 0.6 ‰, which was ~6 ‰ higher than that of ... [8]

Formatted: Font: 12 pt, Font color: Auto

Formatted ... [9]

Deleted: portend

Deleted: sensitivity

Deleted: dependence

Deleted: ... This...factor shouldneeded to ... [11]

Deleted: to on regional food web structure. This depende ... [12]

Formatted: Font: 12 pt, Font color: Auto

Formatted ... [10]

Deleted: heeded

Deleted: in

Formatted: Font: 12 pt, Font color: Auto

1 Introduction

Interactions between ocean circulation and nutrient cycling modulate the marine biological carbon pump, the consequent partitioning of CO₂ between atmosphere and ocean, and thus influence planetary climate on centennial to millennial time scales (Sigman and Boyle 2000). The marine nitrogen (N) cycle is highly sensitive to these interactions, such that knowledge of modern and ancient ocean N cycling can help illuminate drivers of past climate and contextualize modern global change (e.g., Altabet et al., 1994; Francois et al., 1997; Robinson and Sigman 2008; Sigman et al., 1999; Kast et al. 2019).

The main tool to investigate the oceanic N cycle history is the nitrogen (N) isotope composition (*i.e.*, the ¹⁵N/¹⁴N ratio) of particulate organic nitrogen (PON) exported from the euphotic zone and preserved in various paleo-archives, including bulk sedimentary N in anoxic sediments (reviewed by Robinson et al. 2023). Hereafter, we express the ¹⁵N/¹⁴N ratio in delta notation, where $\delta^{15}\text{N} (\text{‰ vs. air}) = \left[\frac{^{15}\text{N}/^{14}\text{N}_{\text{sample}}}{^{15}\text{N}/^{14}\text{N}_{\text{air}}} - 1 \right] * 1000$. The $\delta^{15}\text{N}$ -PON recorded in paleo-oceanographic archives reflects both regional N cycling processes and the balance of global ocean N source and sink terms (Sigman and Fripiat 2019; Brandes and Devol 2002). In regions of the ocean where nitrate is quantitatively consumed, the annually integrated $\delta^{15}\text{N}$ -PON exported from the surface reflects the isotopic composition of thermocline nitrate (Altabet et al. 1991). The latter is influenced by the circulation history of nitrate (e.g., Marconi et al., 2015), by regional N₂ fixation (e.g., Casciotti et al. 2008; Knapp et al. 2008) and by water column denitrification (e.g., Pride et al., 1999; De Pol-Holz et al., 2007). In regions with incomplete consumption of surface nitrate, such as Southern Ocean, the isotopic discrimination imparted during nitrate assimilation is reflected in the $\delta^{15}\text{N}$ -PON, which can be used to reconstruct the degree of surface nitrate consumption in the past (e.g., Sigman et al., 1999; Francois et al. 1997).

Accurate interpretation of the N cycle's paleo-history relies on the presumption that the $\delta^{15}\text{N}$ -PON preserved in various palaeoceanographic archives is impervious to organic matter diagenesis. Bulk sedimentary $\delta^{15}\text{N}$ measurements are thus generally inadequate in this respect, subject to post-depositional processes (Robinson et al. 2012) – barring fast-accumulating organic-rich anoxic sediments with negligible contribution from terrestrial sources (e.g., Altabet et al., 2002; Ganeshram and Pedersen, 1998). To circumvent this limitation, several “biological” archives of the $\delta^{15}\text{N}$ -PON have been developed that are deemed resistant to diagenetic alteration. These include the organic matter in diatom frustules and foraminifera tests (e.g., Ren et al., 2009; Robinson and Sigman, 2008) and the organic matter in proteinaceous corals (e.g., Sherwood et al. 2009; Williams and Grottooli 2010). Recently, the $\delta^{15}\text{N}$ of organic N enclosed within the aragonite mineral lattice of asymbiotic scleractinian (stony) cold-water corals (CWCs) has been found to reflect the $\delta^{15}\text{N}$ -PON exported from the surface

Deleted:

Formatted: Font color: Text 1

Deleted: and

Deleted: , organic N in in soft corals, and organic N material preserved in foraminiferal tests and in diatom frustules

Deleted: Henceforth

Formatted: Font color: Text 1

Deleted: :

Formatted: Font color: Text 1

Formatted: No underline, Font color: Text 1

Formatted: Font color: Text 1

Formatted: No underline, Font color: Text 1

Formatted: Font color: Text 1

Formatted: No underline, Font color: Text 1

Formatted: Font color: Text 1

Formatted: Font color: Text 1

Deleted: intercalated

138 ocean (Wang et al., 2014), offering an exciting new archive of marine N cycling (Wang et al. 2017; Li et al.,
 139 2020, Studer et al., 2018; Chen et al. 2023). A robust cold-water coral archive of $\delta^{15}\text{N}$ -PON can complement the
 140 existing suite of nitrogen proxies by reducing the potential biases inevitable for almost any individual proxy,
 141 allowing for a broader geographic and temporal reconstruction, and increasing resolution of the proxy record.
 142 Foremost, as with foraminifera and diatom shells, organic material trapped within the coral's original aragonite
 143 mineral lattice is largely protected from diagenetic alteration (Drake et al. 2021), and compromised areas can be
 144 avoided by inspecting the skeletons for contamination and recrystallization (e.g., borings) using microscopic
 145 techniques (Gothmann et al. 2015). CWCs have a broad geographic distribution, being present in all ocean basins
 146 from the surface to 5000 m (Freiwald, 2002). CWCs also offer the potential to generate high-resolution records
 147 extending relatively far back in time, and corals have continuous skeletal accretion that records ocean conditions
 148 at the time of growth, so the analysis of multiple individuals provides enhanced temporal resolution of long-time
 149 record (Robinson et al., 2014; Hines et al. 2015). Unlike sediments containing microfossils (e.g. diatoms and
 150 foraminifera) CWC skeletons are not subject to bioturbation and absolute ages of this paleoarchive can be
 151 determined with decadal precision on the time scales of glacial-interglacial climate variability through U-Th
 152 series dating (Cheng et al., 2000; Goodfriend et al. 1992, Robinson et al., 2014, Li et al., 2020). Remarkably,
 153 individual coral samples can archive multiple seawater properties, such that a single CWC specimen can
 154 potentially be used to reconstruct deep (e.g., $\Delta^{14}\text{C}$, pH, temperature, and circulation proxies such as Ba/Ca
 155 and ϵNd) and surface ocean conditions ($\delta^{15}\text{N}$) at a precisely-known time (U-Th dating), making CWC unique as a
 156 paleoceanographic archive (Robinson et al., 2014; Thiagarajan et al., 2014; Rae et al. 2018).
 157 Yet an outstanding concern about the fidelity of the $\delta^{15}\text{N}$ of coral-bound organic N is a reported 8 - 9 ‰
 158 offset between coral-bound $\delta^{15}\text{N}$ and the corresponding $\delta^{15}\text{N}$ -PON exported to regions of coral growth (Wang et
 159 al. 2014). The magnitude of this offset substantially exceeds the 3 - 3.5 ‰ expected for a single trophic transfer
 160 (Minagawa and Wada 1984), assuming CWC feed predominantly on algal material exported from the surface
 161 ocean, Wang et al. (2014) explained the magnitude of the offset by arguing that CWCs feed on the more
 162 abundant pool of surface-derived suspended organic material (SPOM), as the $\delta^{15}\text{N}$ SPOM at depth is typically
 163 ~4-5‰ higher than that of sinking PON (Altabet 1988, Saino and Hattori, 1987). While CWCs are considered
 164 generalists with regard to diet (e.g., Mortensen, 2001; Freiwald, 2002; Carlier et al., 2009; Maier et al. 2023), a
 165 number of studies suggest that many species of CWC subsist predominantly on metazoan zooplankton prey (e.g.,
 166 Naumann et al. 2011; Kiriakoulakis et al. 2005; Purser et al. 2010; Tsounis et al. 2010). A zooplankton diet
 167 should result in an approximate two-level or more trophic transfer between surface PON and coral tissue (e.g.,

Formatted: Font color: Text 1

Formatted: Font color: Text 1

Deleted: almost

Deleted: each

Formatted: Font color: Text 1

Deleted: presumably

Formatted: Font color: Text 1

Deleted: .

Deleted: ;

Deleted: Coral skeletons can also be

Deleted: ed

Deleted: to avoid compromised areas

Deleted: They

Deleted: are

Deleted: thus

Deleted: directly dated with radiometric methods;

Formatted: Font color: Text 1

Formatted: Font color: Text 1

Formatted: Font color: Text 1

Deleted: Despite its promise,

Formatted: Font color: Text 1

Deleted: were

Deleted: assuming that

Deleted: to

Deleted: (Duineveld et al. 2007; 2012)

Deleted: reconciled this observation

Deleted: of which

Deleted: exported from the surface

Deleted:

Deleted: Duineveld et al. 2004; 2007; 2012; Kiriakoulakis et al. 2005, ...

Deleted: , Dodds et al., 2009; van Oevelen et al. 2009

Formatted: No underline, Font color: Text 1

Formatted: Font color: Text 1

Formatted: Font color: Text 1

Deleted: ; Carlier et al. 2009; Dodds et al. 2009;

Deleted: van Oevelen et al. 2009;

194 Sherwood et al. 2008), ~~closer~~ to the observed 8-9 ‰ offset, potentially rendering coral-bound $\delta^{15}\text{N}$ sensitive to
195 spatial and temporal differences in ~~trophic-level~~ food web structure. An alternative explanation for the offset is
196 that there is a large biosynthetic offset between the $\delta^{15}\text{N}$ of the CWC polyp and its skeletal tissue (Horn et al.
197 2011; Muscatine et al. 2005), assuming that CWCs' diet derives directly from sinking algal material from the
198 surface ocean. Otherwise, there could be an atypically large N isotope fractionation associated with the trophic-
199 level transfer between the coral diet and its tissue (>3-3.5‰), possibly borne out of intermittent starvation periods
200 (Doi et al., 2017), which is then ~~passed on~~ to the organic matrix within the coral skeleton. The gap in our
201 understanding of how corals record the $\delta^{15}\text{N}$ -PON exported from the surface ocean raises questions regarding the
202 consistency of the offset in space and time, and whether it is ~~likely~~ to differ among CWC species or due to intra-
203 specific variations in diet.

204 Due to the challenges of accessing deep ocean environments, the trophic ecology of cold-water corals is
205 sparsely documented, yet is fundamental to understanding the role of CWCs in cold-water reef ecosystems and to
206 defining their utility as paleoceanographic archives of N cycling. The nature of the $\delta^{15}\text{N}$ offset between CWC
207 skeletal material and exported PON must be explained in order to ~~further validate and potentially improve~~ the use
208 of ~~$\delta^{15}\text{N}$ of CWC skeletons as a proxy~~ to reconstruct the history of exported PON and to further understand the
209 role of CWCs in benthic ecosystems. To this end, we studied *Balanophyllia elegans*, an ~~asymbiotic~~ scleractinian
210 cold-water coral found along the west coast of North America that grows as individual polyps (Fadlallah, 1983).
211 We investigated the following questions: a) Is there a large offset in $\delta^{15}\text{N}$ between coral polyp tissue and coral
212 skeletal tissue? b) Is there an unusually large trophic-level offset between coral tissue and coral diet? c) Does *B.*
213 *elegans* feed predominantly on suspended particulate organic matter (SPOM) *in situ*? or d) does *B. elegans* feed
214 predominantly on metazoan zooplankton, resulting in a two-level trophic transfer between coral tissue and N of
215 export? To evaluate question (a), ~~we measured the $\delta^{15}\text{N}$ of tissue-skeleton pairs of coral samples collected in their~~
216 ~~natural habitat~~. To evaluate question (b), we cultured *B. elegans* corals in the laboratory ~~in experiments where~~
217 ~~both the isotopic composition of food and the frequency of feeding was controlled~~. To evaluate questions (c) and
218 (d), ~~we also investigated the $\delta^{15}\text{N}$ of various~~ components of the food web at a field site ~~where *B. elegans* are~~
219 ~~found plentifully~~. Our observations offer novel insights on the growth and trophic ecology of *B. elegans*,
220 providing unique new data on the N metabolism of CWC and their feeding ecology. We contextualize our
221 conclusions to inform the use of CWC archives as a paleo-proxy for marine N cycling and ocean
222 biogeochemistry.

223

Deleted: similar

Deleted: and

Deleted: lower

Deleted: communicated

Deleted: apt

Formatted: Font color: Text 1

Deleted:

Deleted:

Formatted: Font color: Text 1

Deleted: fully

Formatted: Font color: Text 1

Deleted:

Deleted:

Deleted: s

Deleted:

Deleted: ies

Formatted: Font color: Text 1

Formatted: Font color: Text 1

Deleted: s

Deleted:

Formatted: Font color: Text 1

Deleted: these

Deleted: s

Deleted: ,

Deleted: naturally-

Deleted: habitats

Deleted: under a controlled diet

Formatted: Font color: Text 1

Deleted: to document trophic isotope effects and soft tissue N turnover, ...we investigated the soft vs. skeletal tissue $\delta^{15}\text{N}$ of coral we investigated the soft vs. skeletal tissue $\delta^{15}\text{N}$ of coral specimens collected from a field site in the Salish Sea, and

Deleted: we investigated the soft vs. skeletal tissue $\delta^{15}\text{N}$ of coral collected from a field site in the Salish Sea, and

Deleted: w

Deleted: queried

Deleted: the

Formatted: Font: Not Italic, Font color: Text 1

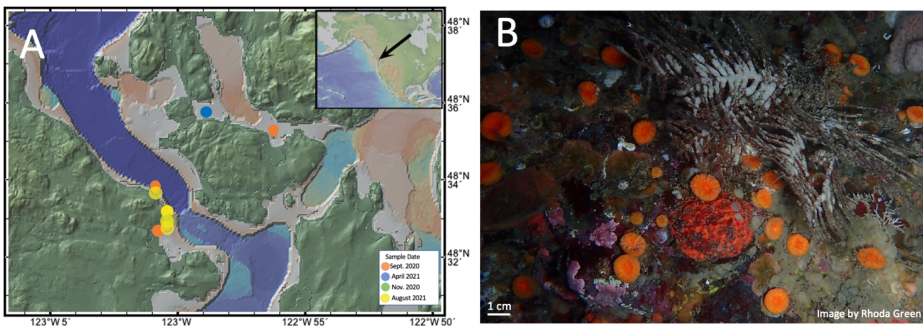
Deleted: .

Formatted: Font color: Text 1

255 2. Methods

256 2.1 Collection of live coral specimens

257 Individual specimens of the cold-water coral *Balanophyllia elegans* were collected during four sampling
258 campaigns in March and June 2019, and September and November 2020 from the San Juan Channel near the
259 University of Washington's Friday Harbor Laboratory off the coast of Washington State in the Salish Sea (48.5°
260 N, -123.0° W; Figure 1). *B. elegans* is a solitary, asymbiotic cold-water cup coral native to the Pacific Northwest
261 that can be found both in shallow rocky environments and at depths as great as 500 m (Durham and Barnard
262 1952). The genus *Balanophyllia* is cosmopolitan and fossil samples as old as Eocene in age have been used for
263 paleoenvironmental study (Muhs et al. 1994; Gothmann et al., 2015; Gagnon et al. 2021). *B. elegans*'s presence
264 at near surface depths makes it an easy target for culture experiments, and *Balanophyllia* sp. can be found co-
265 occurring with the similar but more widely applied cold-water coral archive, *Desmophyllum dianthus* (Margolin
266 et al. 2014). Therefore, we consider the asymbiotic *Balanophyllia* sp. to be generally representative of other deep
267 cold-water coral species.



268 Figure 1. (a) Map of the San Juan Islands indicating the collection site of *B. elegans* specimens and
269 hydrographic measurements (created using <http://www.geomapapp.org>, Ryan et al. 2009). Inset shows
270 where the San Juan Islands are situated within North America. (b) Image of *B. elegans* from the San
271 Juan Channel near Friday Harbor Labs taken by Rhoda Green.

B. elegans specimens were collected at 10 to 20 m depth by divers who gently removed the corals from
vertical rock walls using blunt-tipped diving knives. Of the live corals collected, a subset was immediately frozen
at -18°C for N isotope ratio analyses of soft tissue and organic matter bound in the coral skeleton matrix. Live
specimens were shipped overnight in small bags of seawater on ice to St. Olaf College (Minnesota, USA). Corals

Formatted: Font color: Text 1

Formatted: Font color: Text 1

Deleted: depths

Deleted: the

Deleted: but

Formatted: Font color: Text 1

Formatted: Font: (Default) +Headings (Times New Roman),
Font color: Text 1

Formatted: Font: (Default) +Headings (Times New Roman)

Formatted: Line spacing: single

Deleted: ESRI, 2021

Formatted: Font: (Default) +Headings (Times New Roman),
Font color: Text 1

Formatted: Font: 11 pt, Not Bold, Font color: Text 1

Formatted: Font: 11 pt, Not Bold, Font color: Text 1

Formatted: Font color: Text 1

Formatted: Font: (Default) +Headings (Times New Roman)

Deleted: S

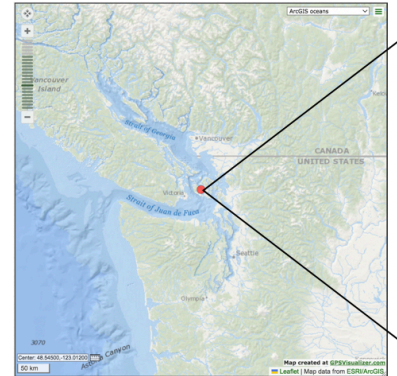
Formatted: Indent: First line: 0.25", Line spacing: 1.5 lines

276 were cleaned by gently scraping the exposed skeleton with dental tools to remove encrusting organisms and
277 placed in incubation bottles with artificial seawater for recovery prior to feeding experiments (described below).

278 2.2 Live coral maintenance

279 Live *B. elegans* corals were maintained in artificial seawater medium prepared from nitrate-free Instant
280 Ocean® Sea Salt. Salts were dissolved in deionized water to a salinity of 28.0 ± 0.25 – akin to the conditions at
281 the collection site (Murray et al., 2015) – and sparged with air to achieve atmospheric equilibrium. The pH of the
282 seawater was measured with a YSI brand 4130 pH probe and adjusted using dilute (0.1 N) hydrochloric acid or
283 sodium hydroxide to 8.14 ± 0.05 , slightly higher than *in-situ* conditions to promote skeletal growth. Batch
284 seawater was then allotted to 2 L airtight polypropylene bottles to incubate single coral polyps. Bottles were pre-
285 cleaned with fragrance-free soap and multiple rinses of deionized water. The salinity, pH, and temperature in the
286 incubation bottles were monitored using YSI brand probes (4310(W) conductivity cell and pH probe,
287 respectively) as well as dissolved oxygen concentrations using an optical sensor (FDO 4410; Figure S1); a
288 Multilab 4010-3w was used as the digital meter for the sensors. The bottles containing individual corals were
289 randomly distributed among three recirculating water baths maintained at a constant temperature of 12.5 ± 0.2 °C,
290 akin to the conditions at the collection site (Murray et al., 2015). Small but quasi-systematic differences of \pm
291 0.3 °C were observed among the three recirculating tanks (Figure S2). Corals were sustained on a diet of *Artemia*
292 *salina* nauplii (described below), fed twice a week to ensure maximum growth (Crook et al., 2013). Seawater in
293 the incubation bottles was replaced twice a week after the corals were fed, based on observations indicating that
294 seawater pH in the bottles decreased slightly but significantly by ~ 0.03 pH units over three days due to coral
295 respiration (statistical analysis was performed with RStudio; Welch two sample t-test; $t(515.07) = 12.8$; p-value <
296 0.01; Figure S3). Dissolved oxygen concentrations remained near atmospheric equilibrium at concentration of 7.5
297 ± 0.3 mg L⁻¹ (Figure S1). Nitrate concentrations in the bottles were also monitored from samples taken during
298 each water change, in the freshly prepared seawater and in spent seawater, revealing low variability in NO₃⁻
299 concentration of 0.7 ± 0.3 μmol L⁻¹ (Figure S4). Nitrate concentrations in the incubations were notably lower than
300 ambient levels at the collection site, where concentration were ~ 25 μmol L⁻¹, ensuring that the coral's only source
301 of nitrogen was the *Artemia* diet (Murray et al., 2015).

Deleted: ¶



Formatted: Font color: Text 1

Formatted: Font color: Text 1

Formatted: Font color: Text 1

Formatted: Font color: Text 1

304 2.3 Coral culture experiments

305 2.3.1 *Experiment to quantify the trophic isotope effect*

306 The corals were acclimated to precise incubation conditions for approximately 20 hours before initiating
307 feeding experiments. To assess the $\delta^{15}\text{N}$ of coral soft tissue compared to that of its food source, four experimental
308 groups of individual *B. elegans* corals were fed respective diets of *Artemia salina* nauplii with different $\delta^{15}\text{N}$
309 values, twice per week for 530 days (Spero et al., 1993). Unhatched *Artemia salina* sourced from specific
310 geographic locations have widely different $\delta^{15}\text{N}$ values, owing to the different N isotope dynamics of the
311 environments from which they were collected, which makes these organisms useful for trophic studies (Spero et
312 al. 1993). Eighteen coral specimens were fed *Artemia* nauplii hatched from cysts from the Great Salt Lake
313 (Reference Code: GSL) with a $\delta^{15}\text{N}$ of 17.0 ± 0.3 ‰. Twelve corals were fed hatched nauplii from Lake Ulzhay
314 in Russia (Reference Code: 1816) with a $\delta^{15}\text{N}$ of 13.8 ± 0.4 ‰. Twelve corals were fed hatched nauplii from
315 Vinh Chau in Vietnam (Reference Code: 1805) with a $\delta^{15}\text{N}$ of 9.9 ± 0.3 ‰. Twelve corals were fed hatched
316 nauplii from Tibet (Reference Code: 1808) with $\delta^{15}\text{N}$ of 6.3 ± 0.2 ‰. The GSL *Artemia* was procured from
317 Aquatic Foods California Blackworm Co. (Great Salt Lake), whereas all other *Artemia* were obtained from the
318 *Artemia* Reference Center (Ghent, Belgium). The $\delta^{15}\text{N}$ of the diet for each treatment was calculated as the mean
319 value measured from each group of unhatched cysts and hatched nauplii (Table S2 and S3).

320 Fresh batches of nauplii were hatched from *Artemia* cysts at approximately monthly intervals, filtered into a
321 concentrated suspension, stored frozen at -18°C , and thawed immediately before feeding to the corals. Due to low
322 hatch rates of the *Artemia* group 1808, corals in that treatment group were fed nauplii harvested from
323 decapsulated *Artemia* cysts from day 151 (November 19, 2019) to 245 (February 22, 2020). The $\delta^{15}\text{N}$ of the
324 hatched nauplii ranged from 6.3 ± 0.2 to 17.0 ± 0.3 ‰ (measured by EA-IRMS; Table S2). The $\delta^{15}\text{N}$ of the
325 nauplii did not change significantly over prolonged storage of several months in the freezer (ANOVA test; $F(1) =$
326 0.07 , $p\text{-value} = 0.80$; Figure S5). *Artemia* nauplii had a statistically indistinguishable molar C:N ratios among
327 regional groups, averaging 6.0 ± 0.6 (ANOVA test; $F(3) = 0.31$; $p\text{-value} = 0.82$, Table S3). These results show
328 that there was limited variability in the diet of corals due to freezer storage and hatching of multiple individual
329 batches of *Artemia* (Table S2, S3, Figure S5).

330 Corals were fed their respective nauplii diets by transferring coral individuals from their incubation bottle to
331 a small dish filled with artificial seawater with minimal exposure to air so as not to stress the corals. Each coral
332 was fed 20 μL of thawed nauplii suspension by pipetting the food directly into their oral cavity, making it
333 possible to visually ensure complete consumption and thus minimize variability in feeding rates. Each coral was

Deleted: Evaluation of the trophic isotope effect and turnover time

Formatted: Font color: Text 1

Deleted: We refer to respective experimental groups by a color name (green, yellow, orange and pink).

Deleted: assigned to the green group

Deleted: The yellow group consisted of t

Deleted: that

Formatted: Font color: Text 1

Deleted: in the orange group which was

Formatted: Font color: Text 1

Deleted: The pink group consisted of t

Deleted: that

Formatted: Font color: Text 1

Formatted: Font color: Text 1

Formatted: Font color: Text 1

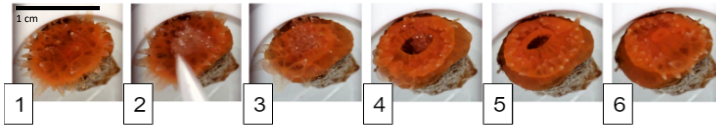
Deleted: 3

Formatted: Font color: Text 1

Formatted: Line spacing: 1.5 lines

345 returned to its bottle with a fresh allotment of seawater when its mouth had remained closed for several minutes,
346 signifying that it was finished eating (Figure 2).

347 After a shift in the $\delta^{15}\text{N}$ of diet, it is expected that coral tissue $\delta^{15}\text{N}$ will evolve as a function of time until the
348 composition of tissue reaches an equilibrium in line with the new diet. In order to assess the rate (referred to here
349 as the isotopic turnover time) at which this evolution occurs, individual corals were sacrificed at discrete intervals
350 throughout the experiment. Corals were always sacrificed three days after feeding to ensure that no food
351 remained in the oral cavity. The corals were removed from their bottles and rinsed with artificial seawater. The
352 coral tissue was then separated from the skeleton using a fine stream of compressed air. The tissue and skeleton
353 were frozen at -18°C and stored separately until processed for isotope ratio analyses.



347 **Figure 2.** Photo illustration of a coral feeding sequence. Photo 1 shows coral before food is given. Photo 2
348 shows food being pipetted onto coral mouth. Photos 3 through 6 show the coral feeding as the mouth opens to
349 engulf food and closes when finished, about 15 minutes in total. Corals are ~1 cm in diameter.

354 2.3.2 Experiment to evaluate the effects of starvation conditions

355 An additional 522-day feeding experiment was performed to assess the influence of starvation on the $\delta^{15}\text{N}$ of
356 the coral soft tissue. Live corals collected during a sampling campaign at the end of November 2020 and shipped
357 live to St. Olaf College were randomly assigned to two treatment groups (starved and not-starved). Corals in the
358 starved treatment were fed at 25% of our normal feeding frequency, or every two weeks, whereas those in the
359 not-starved treatment were fed twice a week. These feeding regimes were chosen based on the work of Crook et
360 al. (2013) and Beauchamp et al. (1989), who assumed feeding every 3 days to represent plentiful food supply and
361 feeding every 21 days (close to our starvation condition) to represent minimal maintenance food supply. Both
362 groups were fed *Artemia* nauplii with a $\delta^{15}\text{N}$ of 9.9 ± 0.3 ‰, approximately 3 ‰ lower than the coral tissue of
363 average *B. elegans* collected from Friday Harbor, and thus presumably closest in $\delta^{15}\text{N}$ to what the corals is eating
364 in the wild given a canonical trophic isotope effect. Coral incubations and feedings were conducted as described
365 above. Individuals were sacrificed over the course of the 522-day experiment, and tissue samples were frozen at
366 -18°C until isotope analysis.

Formatted: Font color: Text 1

Formatted: Font color: Text 1

Formatted: Font color: Text 1

Moved (insertion) [2]

Formatted: Font color: Text 1

Formatted: Font color: Text 1

Moved up [2]: Corals were always sacrificed three days after feeding to ensure that no food remained in the oral cavity. The corals were removed from their bottles and rinsed with artificial seawater. The coral tissue was then separated from the skeleton using a fine stream of compressed air. The tissue and skeleton were frozen at -18°C and stored separately until processed for isotope ratio analyses.

Moved (insertion) [1]

Deleted: Individual corals were sacrificed at discrete intervals throughout the experiment to monitor N turnover. Corals were always sacrificed three days after feeding to ensure that no food remained in the oral cavity. The corals were removed from their bottles and rinsed with artificial seawater. The coral tissue was then separated from the skeleton using a fine stream of compressed air. The tissue and skeleton were frozen at -18°C and stored separately until processed for isotope ratio analyses.

Deleted: ¶

¶

Deleted: In order to determine the trophic $\delta^{15}\text{N}$ offset between tissue and prey and to estimate the turnover time of the coral tissue with respect to nitrogen, we fit the data to a least-squares regression corresponding to an isotope mixing model in which describes the time-dependent evolution of tissue $\delta^{15}\text{N}$ in relation to that of the diet (Eq. 1, after Cerling et al. 2007; Ayliffe et al. 2004), ¶

$$N = N_{\text{diet}} + \epsilon \cdot e^{-\lambda t}$$

The term $\delta^{15}\text{N}_{\text{diet}}$ is the value of the coral tissue at the onset of the experiment, $\delta^{15}\text{N}_{\text{diet}}$ is that of the corals' *Artemia* diet, t is the number of days since the start of the experiment, ϵ is the difference between the $\delta^{15}\text{N}$ of the diet and tissue at equilibrium, and λ is the specific nitrogen incorporation rate (d^{-1}), the inverse of which is the turnover time for N. Values of ϵ and λ were estimated by generating 4 simultaneous equations using the $\delta^{15}\text{N}$ of soft tissue and diet for the 4 treatments groups. ¶

Deleted: E

Deleted: ion of

Formatted: Font color: Text 1

Deleted: , referred to as "long" and "short".

Deleted: "long"

Deleted: weeks,

Deleted: "short"

405 2.4 Coral preparation for isotope ratio analyses

406 Frozen coral tissue samples (and hatched nauplii) were freeze-dried using a Labconco FreeZone 4.5 and then
407 powdered using a mortar and pestle. The samples were sent to the University of Connecticut, Avery Point
408 (Groton, CT, USA) for isotope ratio analyses.

409 Coral skeletons from specimens collected at Friday Harbor were separated from the coral soft tissue and were
410 rinsed and individually ultrasonicated two times in Milli-Q™ (MQ) water for 20 minutes each in order to
411 remove any residual seawater. Samples were then individually ultrasonicated in a 1% sodium hypochlorite
412 (bleach) solution for at least two 20-minute intervals with fresh bleach for each new ultrasonication interval until
413 no tissue remained on the skeleton, as assessed visually under a dissection microscope. Individual skeletons were
414 then rinsed and ultrasonicated for 20 minutes in MQ another three times (each time with a new batch of MQ
415 water) in order to remove any bleach residue. Skeleton samples were sent to Pomona College (California, USA)
416 for further processing.

417 It is necessary to isolate organic matter from the coral carbonate matrix in advance of the N isotope
418 measurement methods used here (see Section 2.6 below). Organic material in the skeleton matrix was isolated
419 and oxidized to nitrate following the protocol of Wang et al. (2014). Briefly, bulk samples weighing 50-100 mg
420 were ground into coarse powder, and a fraction between 63 and 200 μm was collected by sieving through two
421 metal sieves. The 10-15 mg of sieved powder was rinsed sequentially with of sodium polyphosphate-sodium
422 bicarbonate buffered dithionite-citrate reagent, then treated with 13.5% sodium hypochlorite overnight on a
423 shaker. Skeletal material was dissolved in 4 N ultrapure hydrochloric acid, then oxidized to nitrate by autoclaving
424 in basic potassium persulfate solution. Standards of glutamine reference material USGS-40 and USGS-41
425 (respective δ¹⁵N of 4.52 ‰ vs. air and 47.57 ‰ vs. air) were oxidized in tandem and used to correct for
426 processing blanks. The resulting nitrate samples were sent to the University of Connecticut for nitrate isotope
427 ratio analysis. The long-term averaged reagent blank was 0.4-0.6 μmol L⁻¹, while the typical samples were 10-15
428 μmol L⁻¹ (typical amount of nitrogen in skeleton being 2-5 μmole/g of aragonite). Samples were typically run in
429 duplicates with an average reproducibility of ~ ± 0.5 ‰. An internal laboratory standard of ground material of the
430 cold-water colonial scleractinian coral *Lophelia pertusa* had a long-term δ¹⁵N value 9.4 ± 0.8 ‰ (n=57)

431 2.5 Hydrographic data

432 To infer the natural food source of the *B. elegans*, we collected samples for analysis of the δ¹⁵N of particulate
433 and dissolved N pools in relation to ambient hydrographic variables (temperature and salinity) near Friday

Formatted: Font color: Text 1

Deleted: separate

Deleted: .

Deleted: .

Formatted: Font color: Text 1

Formatted: Font color: Text 1

Formatted: Font color: Text 1

Formatted: Font color: Text 1

Formatted: Font color: Text 1

Deleted: .

Deleted:

Formatted: Font color: Text 1

Formatted: Font color: Text 1

Deleted:

Deleted: 8.8

Deleted: 1.2

Deleted: 106

Formatted: Font color: Text 1

Formatted: Font color: Text 1

Formatted: Font color: Text 1

443 Harbor, WA. Seasonal sampling campaigns were conducted in September and November 2020 and in April,
444 June, and August 2021 (Table S1). In all but the August 2021 campaign, particulate and dissolved N samples
445 were collected by divers at unspecified depths between the surface and the depth of coral collection. Samples
446 were stored frozen in 30 mL HDPE bottles. Surface net tows were performed with a mesh size of 120 μm ;
447 materials were stored and shipped frozen and thawed at a later time to be filtered onto pre-combusted GF/F filters
448 (0.7 μm nominal pore size) that were stored frozen pending isotope analysis. No hydrographic variables were
449 recorded during the campaigns except in August 2021.

450 During the August 2021 campaign, depth profiles of temperature and salinity from the surface to 35 m were
451 characterized with a CastAway®-CTD (conductivity temperature depth) profiler. Water samples were collected
452 at 5 m intervals between 5 and 30 m using a Van Dorn water sampler. Water was filtered onto pre-combusted
453 glass fiber filters (GF/F; 0.7 μm nominal pore size) into pre-cleaned 30 mL HDPE bottles and stored frozen
454 pending analyses of nitrate concentrations and nitrate isotope ratios. The corresponding filters were stored frozen
455 for isotope ratio analysis of suspended particulate organic material (SPOM). Surface (5 m) and deeper (25 m to
456 the surface) net tows were conducted using plankton nets with respective mesh sizes of 150 μm and 80 μm . Net
457 tow material was filtered directly onto a pre-combusted GF/F filters and frozen pending analysis. A portion of the
458 net tow material from the August 2021 campaign was sieved to separate size classes of 80-100 μm , 100-250 μm ,
459 $\geq 250\mu\text{m}$, 250-500 μm , and $\geq 500 \mu\text{m}$. Material from the respective size classes was filtered onto pre-combusted
460 GF/F filters and frozen until isotope analysis.

461 2.6 Nitrate concentrations and isotope ratio analyses

462 Nitrate concentrations of oxidized coral skeletons and in aqueous samples were measured by reduction to
463 nitric oxide in hot vanadium III solution followed by chemiluminescence detection of nitric oxide (Braman and
464 Hendrix, 1989) on a Teledyne chemiluminescence NOx analyzer Model T200 (Thousand Oaks, CA).

465 The $\delta^{15}\text{N}$ and $\delta^{13}\text{C}$ of lyophilized coral tissue samples were analyzed at the University of Connecticut on a
466 Costech Elemental Analyzer–Isotope Ratio Mass Spectrometer (Delta V). Approximately 0.75 mg of lyophilized
467 sample (35 μg N) was allotted into tin cups and analyzed in tandem with recognized glutamine reference
468 materials USGS-40 and USGS-41 with respective $\delta^{15}\text{N}$ (vs. air) of 4.52 ‰ and 47.57 ‰ and $\delta^{13}\text{C}$ of -26.39 ‰
469 and 37.63 ‰ (vs. PDB). Replicate analyses of ($n \geq 2$) reference materials yielded an analytical precision of (± 1
470 SD) of 0.3 ‰ for both $\delta^{15}\text{N}$ and $\delta^{13}\text{C}$.

Deleted: undefined

Formatted: Font color: Text 1

Formatted: Line spacing: 1.5 lines

Commented [AMG1]: Agreed. This seems wrong.

Commented [JM2R1]: Julie can you double check this

Deleted: 5

Formatted: Font color: Text 1

Formatted: Font color: Text 1

473 Nitrate N (and O) isotope ratios of aqueous seawater samples and N isotope ratios of the skeleton matrix
474 samples were analyzed at University of Connecticut using the denitrifier method (Casciotti et al., 2002; McIlvin
475 and Casciotti, 2011; Sigman et al., 2001). Nitrate sample solutions were injected at target concentrations of 20
476 nmol for seawater samples and 7 nmol for skeleton matrix samples. N₂O was extracted, concentrated and purified
477 using a custom-modified Thermo Gas Bench II equipped with a GC Pal autosampler and dual cold traps and
478 analyzed on a Thermo Delta V Advantage continuous flow isotope ratio mass spectrometer (Casciotti et al., 2002;
479 McIlvin and Casciotti, 2011). Individual analyses were referenced to injections of N₂O from a pure gas cylinder
480 and standardized through comparison potassium nitrate reference materials International Atomic Energy Agency
481 nitrate (IAEA-N3) and the isotopic nitrate reference material United States Geological Survey 34 (USGS-34),
482 with respective $\delta^{15}\text{N}$ vs. air of 4.7 ‰ and -1.8 ‰ vs. air (International Atomic Energy Agency, 1995), and
483 respective $\delta^{18}\text{O}$ of 25.61 ‰ and -27.9 ‰ vs. Vienna Standard Mean Ocean Water (VSMOW; Gonfiantini, 1995;
484 Böhlke et al., 2003). To account for bacterial blanks and source linearity, nitrate concentrations of the standard
485 material – diluted in N-free seawater for aqueous seawater samples and air-equilibrated milli-Q water for
486 skeleton matrix samples – were matched to those of samples within batch analyses, and additional bacterial
487 blanks were also measured (Weigand et al., 2016; Zhou et al., 2022). Replicate measurements ($n \geq 2$) of all
488 samples yielded an average analytical precision (± 1 SD) of 0.3‰ for both $\delta^{15}\text{N}$ and $\delta^{18}\text{O}$.

Formatted: Line spacing: 1.5 lines

Formatted: Font color: Text 1

Formatted: Font color: Text 1

Formatted: Font color: Text 1

Deleted: es

Deleted: es

Deleted: The denitrifier method uses denitrifying bacteria (*Pseudomonas chlororaphis* f. sp. *aureofaciens*, ATCC 13985) that lack the terminal nitrous oxide (N₂O) reductase to quantitatively convert nitrate to nitrous oxide which is measured by gas-chromatography-isotope ratio mass spectrometry. Cells were cultured in Tryptic Soy Broth (Difco; Hunt Valley, MD, USA) amended with 10 mM nitrate in stoppered glass bottles. Cells in stationary phase were harvested by centrifugation and resuspended in nitrate-free medium and dispensed as 3 mL aliquots into 10 mL glass vials, which were then sparged with dinitrogen (N₂) gas for approximately 6 hours to remove N₂O. Nitrate sample solutions (20 nmol for seawater samples and 7 nmol for skeleton matrix samples) were injected into the sparged vials and incubated overnight to allow for complete conversion of nitrate to N₂O gas.

Deleted: ¶

Deleted: The product

Formatted: Font color: Text 1

Formatted: Font color: Text 1

Formatted: Font color: Text 1

Formatted: Font color: Text 1

Deleted: ¶

¶

¶

Formatted: Font color: Text 1

511 **3. Results**

512 3.1 Trophic isotope effect

513 At the onset of the culture experiment, the soft tissue among all experimental corals had a $\delta^{15}\text{N}$ of 11.7 ± 0.5
514 %. Over the course of the experiment, the $\delta^{15}\text{N}$ of the tissue increased or decreased in respective treatments
515 depending on the $\delta^{15}\text{N}$ of their *Artemia* diet (Figure 3); the tissue $\delta^{15}\text{N}$ increased in corals fed diets with $\delta^{15}\text{N}$
516 values of 17.0, 13.8, and 9.9 ‰, whereas the tissue $\delta^{15}\text{N}$ decreased for the diet of 6.4 ‰. The $\delta^{15}\text{N}$ of soft tissue
517 in all groups trended towards an asymptotic offset relative to the diet $\delta^{15}\text{N}$, as expected for an approach to a new
518 equilibrium. However, at day 530, at the end of the experiment, it appeared as though the coral tissue $\delta^{15}\text{N}$ had
519 not yet reached a constant offset value, suggesting that the coral tissue had not yet reached an equilibrium with
520 the new diet. Specifically, at the end of the experiment, the coral tissue of the treatment groups reached $\delta^{15}\text{N}$
521 values of $9.4 \pm 0.3\text{‰}$, $12.6 \pm 0.5\text{‰}$, $15.9 \pm 0.1\text{‰}$, and $18.1 \pm 0.1\text{‰}$ for groups fed the lowest to highest *Artemia*
522 $\delta^{15}\text{N}$ values, respectively. The difference between coral soft tissue and diet $\delta^{15}\text{N}$ ranged from a minimum of $1.0 \pm$
523 0.1‰ to a maximum of $3.0 \pm 0.3\text{‰}$ across the different experimental groups at day 530 (Figure 3).

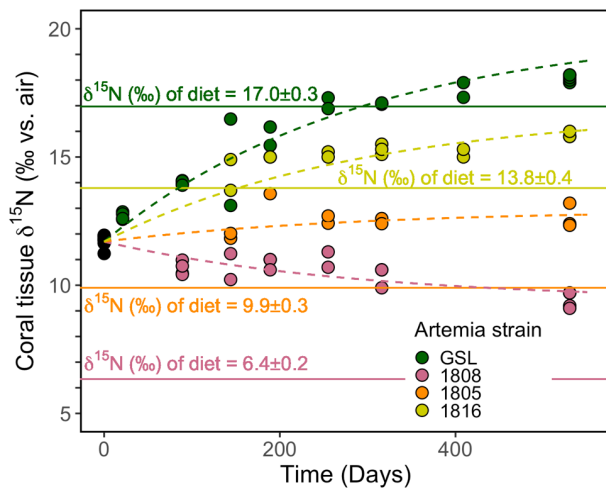


Figure 3. Evolution of the coral soft tissue $\delta^{15}\text{N}$ in response to diet $\delta^{15}\text{N}$. Colors correspond to the respective *Artemia* strains. Dashed lines are the model output of our simultaneous nonlinear least squares regression fits to the data using Equation 1. Solid lines mark the diet $\delta^{15}\text{N} \pm \sigma$. The mean analytical error on tissue $\delta^{15}\text{N}$ analyses was $\pm 0.2\text{‰}$.

528 Despite the fact that coral tissue had not yet reached an equilibrium with the new coral diet at the end of
 529 our experiment, we are able to estimate values of the trophic $\delta^{15}\text{N}$ offset for *B. elegans*, ϵ , and the rate of isotopic
 530 turnover by fitting the data from our trophic isotope experiment to a nonlinear least-squares regression model
 531 corresponding to the isotope mixing relationship shown in Equation 1 below. Equation 1 treats the coral tissue as
 532 a single reservoir of N with some initial isotope composition that is evolving to reflect the new diet as a function
 533 of time (after Cerling et al. 2007; Ayliffe et al. 2004).

$$\delta^{15}\text{N}(t) = [\delta^{15}\text{N}_{t=0} - \delta^{15}\text{N}_{\text{diet}} + \epsilon] \cdot e^{-\lambda t} + \delta^{15}\text{N}_{\text{diet}} + \epsilon. \quad \text{Equation 1}$$

535 The term $\delta^{15}\text{N}_{t=0}$ is the value of the bulk coral tissue at the onset of the experiment, $\delta^{15}\text{N}_{\text{diet}}$ is that of the corals'
 536 new *Artemia* diet (i.e. what it is fed during the experiment), t is the number of days since the start of the
 537 experiment, ϵ is the difference between the $\delta^{15}\text{N}$ of the diet and tissue at equilibrium (i.e. once the isotopic
 538 composition of inputs to the system equals the isotope composition of outputs), and λ describes the specific rate
 539 at which new N is incorporated into the coral tissue (days^{-1}). We use this model to calculate the e-folding time of
 540 the system, which is defined as $1/\lambda$ (days) and represents the time at which ~63% of the original N reservoir in
 541 coral tissue has been replaced with new N from the experimental coral diet.

542 To more confidently calculate ϵ and λ for each individual experimental group, we generate 4 equations,
 543 (one for each experimental group of the form given in Eq. 1 but with different values of $\delta^{15}\text{N}_{\text{diet}}$) and fit them
 544 simultaneously using least-squares regression. From this fit, we are able to obtain estimates for both ϵ and λ in *B.*
 545 *elegans*. An inherent assumption of this approach is that all experimental groups have the same e-folding time
 546 and the same trophic isotope effect. We note here that we refer to the e-folding time as the 'turnover rate' of N in
 547 corals throughout the rest of this text (e.g., Tanaka et al. 2018). Our model fit yielded a trophic isotope effect, ϵ ,
 548 of 3.0 ‰ with a standard error of 0.1 ‰ between coral tissue and diet. The turnover rate of N (i.e. e-folding time,
 549 $1/\lambda$) was 291 days with a standard error of 15 days. The four individual model equations generated by our
 550 nonlinear least squares regression are presented as the dashed lines in Figure 3.

551 3.2 Effect of starvation

552 At the onset of the starvation trial, the coral tissue had an average $\delta^{15}\text{N}$ of 11.5 ± 0.1 ‰. At the end of the
 553 522-day experiment, the starved group (N=15 coral individuals) had an average $\delta^{15}\text{N}$ of 12.4 ± 0.4 ‰ and the
 554 frequently fed group (N=15) with a $\delta^{15}\text{N}$ of 12.7 ± 0.1 ‰ (Figure 4). The starved group was $+2.5 \pm 0.4$ ‰

Formatted ... [13]

Formatted ... [14]

Formatted: Indent: First line: 0.5", Space Before: 4 pt

Deleted: T...is approach assumes ... [15]

Moved up [1]: In order to determine the trophic $\delta^{15}\text{N}$ offset between tissue and prey and to estimate the turnover time of the coral tissue with respect to nitrogen, we fit the data to a least-squares regression corresponding to an isotope mixing model in which describes the time-dependent evolution of tissue $\delta^{15}\text{N}$ in relation to that of the diet (Eq. 1, after Cerling et al. 2007; Ayliffe et al. 2004),

$$N = \dots + \epsilon. \quad \text{Equation 1}$$

The term $\delta^{15}\text{N}_{t=0}$ is the value of the coral tissue at the onset of the experiment, $\delta^{15}\text{N}_{\text{diet}}$ is that of the corals' *Artemia* diet, t is the number of days since the start of the experiment, ϵ is the difference between the $\delta^{15}\text{N}$ of the diet and tissue at equilibrium, and λ is the specific nitrogen incorporation rate (d^{-1}), the inverse of which is the turnover time for N. Values of ϵ and λ were estimated by generating 4 simultaneous equations using the $\delta^{15}\text{N}$ of soft tissue and diet for the 4 treatments groups.

Deleted: Expecting the difference between coral tissue and prey $\delta^{15}\text{N}$ among experimental groups to ultimately converge, corals had evidently not reached isotopic equilibrium relative to prey by the end of the culture experiment. In order to determine the trophic $\delta^{15}\text{N}$ offset between tissue and prey and to estimate the turnover time of the coral tissue with respect to nitrogen, we fit the data to a least-squares regression corresponding to an isotope mixing model in which describes the time-dependent evolution of tissue $\delta^{15}\text{N}$ in relation to that of the diet (Eq. 1, after Cerling et al. 2007; Ayliffe et al. 2004),

$$N = \dots + \epsilon. \quad \dots\text{quation 1}$$

The term $\delta^{15}\text{N}_{t=0}$ is the value of the coral tissue at the onset of the experiment, $\delta^{15}\text{N}_{\text{diet}}$ is that of the corals' *Artemia* diet, t is the number of days since the start of the experiment, ϵ is the difference between the $\delta^{15}\text{N}$ of the diet and tissue at equilibrium, and λ is the specific nitrogen incorporation rate (d^{-1}), the inverse of which is the turnover time for N. Values of ϵ and λ were estimated by generating 4 simultaneous equations using the $\delta^{15}\text{N}$ of soft tissue and diet for the

Deleted: The

Deleted: offset

Deleted: isotopic ...turnover time ...ate of N (i.e. e-folding time, $1/\lambda$) was 291 \pm 15...days with a standard error of 15 days ($\lambda \pm$ standard error) ... [16]

Deleted: also

Deleted:

Deleted: λ

Formatted: Font color: Text 1

635 compared to its diet, statistically indistinguishable from that of the frequently fed group of $+2.8 \pm 0.1$ ‰ higher
636 than the diet (p-value = 0.059, pairwise t-test).

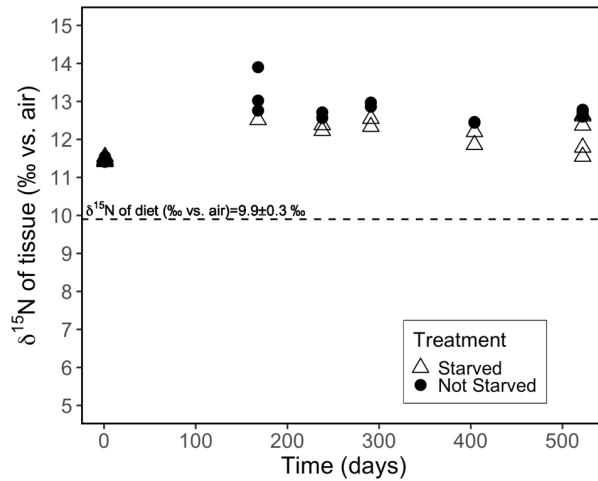


Figure 4. Evolution of the $\delta^{15}\text{N}$ of individual coral polyps fed *Artemia* nauplii ($\delta^{15}\text{N}$ 9.9 ‰) twice weekly (not starved) vs. every two weeks (starved). The analytical error associated with individual tissue $\delta^{15}\text{N}$ measurements was ± 0.2 ‰.

637 3.3 $\delta^{15}\text{N}$ comparison of field specimen polyp tissue and skeleton

638 The $\delta^{15}\text{N}$ of the soft tissue from individual *B. elegans* specimens collected live near Friday Harbor ranged
639 between 11.2 to 13.1 ‰, averaging 12.0 ± 0.6 ‰ (Figure 5a). The soft tissue $\delta^{15}\text{N}$ differed among coral groups
640 collected during different sampling campaigns, with higher values in spring (March 2019 and April 2021)
641 compared to summer and fall (June 2019, September and November 2020; ANOVA $F(4) = 40.39$; p-value ≤ 0.01 ,
642 post-hoc pairwise t-test; p-value < 0.05). The average $\delta^{15}\text{N}$ of corresponding skeletal tissue was 13.5 ± 0.7 ‰ and
643 did not differ discernibly among sampling campaigns (ANOVA $F(2) = 0.916$; p-value = 0.431). The average

Deleted: ; Figure 4

Deleted: ¶

Formatted: Font color: Text 1

Formatted: Font color: Text 1

Formatted: Font color: Text 1

Formatted: Font color: Text 1

Formatted: Line spacing: single

Formatted: Font color: Text 1

Formatted: Left, Indent: First line: 0.5", Space Before: 8 pt, After: 4 pt, Line spacing: 1.5 lines

Deleted: .

649 difference between skeleton and soft tissue $\delta^{15}\text{N}$ ($\Delta\delta^{15}\text{N}$) among coral individuals for which both soft tissue and
 650 skeleton was measured was $1.2 \pm 0.6\%$ (Figure 5b).

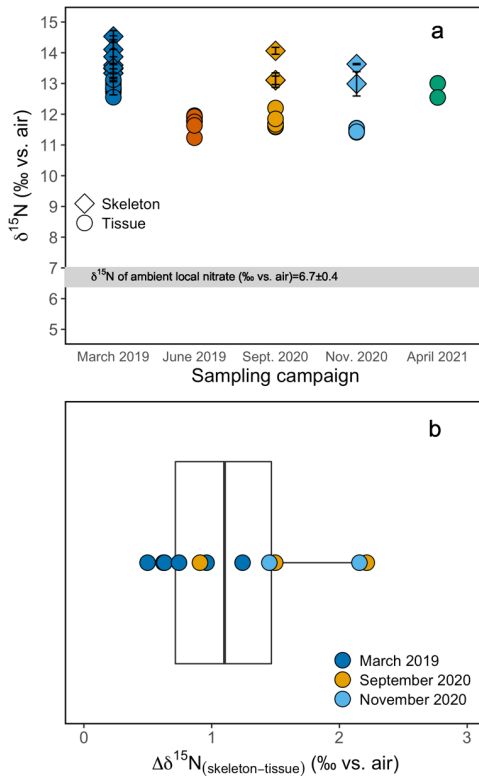


Figure 5. (a) Tissue and skeleton $\delta^{15}\text{N}$ measurements from *B. elegans* individuals collected during different sampling campaigns. Errors on skeleton data are based on replicate analyses of samples from individual polyps. (b) Boxplot of the difference between tissue and skeleton of individual *B. elegans* corals. The boxplot shows the mean, first and third quartile, maxima, and minima. Individual data points are overlaid on the plot. Colors correspond to respective sampling campaigns.

651 3.4 Regional hydrography and N isotope ratios of nitrate and plankton material

652 Hydrographic profiles recorded at stations near Friday Harbor in August 2021 showed characteristic density
 653 structures that were sensitive to tidal phase (Figure 6 a,b; Banas et al. 1999). Profiles collected during flood tide

Commented [JG3]: I find myself not understanding the lines about the "error" in the caption

Deleted: were

Deleted: ¶

Formatted: Font color: Text 1

Formatted: Font color: Text 1

Formatted: Font color: Text 1

Formatted: Font color: Text 1

Formatted: Font color: Text 1

Formatted: Font color: Text 1

Formatted: Indent: First line: 0", Space Before: 0 pt, After: 0 pt, Line spacing: single

Deleted:

Deleted: Errors on skeleton $\delta^{15}\text{N}$ are given in the text.

Deleted: tissue

Deleted: measurements of

Formatted: Font: 11 pt, Font color: Text 1

Formatted: Font: 11 pt, Font color: Text 1

Formatted: Font: 11 pt

Deleted: ¶

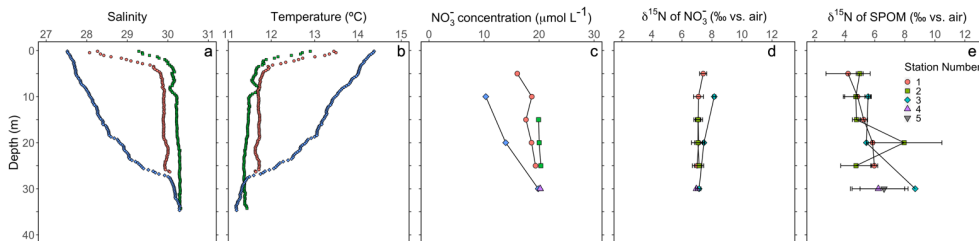
Deleted: Figure 5. (a) Tissue and skeleton $\delta^{15}\text{N}$ measurements from *B. elegans* individuals collected during different sampling campaigns. Errors on skeleton $\delta^{15}\text{N}$ are given in the text. Errors on tissue data are based on measurements of replicate samples. (b) Boxplot of the difference between tissue and skeleton of individual *B. elegans* corals. The boxplot shows the mean, first and third quartile, maxima, and minima. Individual data points are overlaid on the plot. Colors correspond to respective sampling campaigns. ¶

Formatted: Font color: Text 1

665 (collected between 11:40 and 14:20 on August 2, 2021), were relatively well-mixed (salinity 30, temperature
 666 11.8°C), with fresher and warmer water restricted to the near surface (≤ 5 m), whereas ebb-tide profiles (collected
 667 at 9:00 on August 2, 2023) showed a progressive decrease in salinity from 30 to 27 and a corresponding increase
 668 in temperature from 11.8°C at 35 m to 14.5°C at the surface.

669 Nitrate concentrations were nearly uniform with depth during flood tide ($\sim 20 \mu\text{mol L}^{-1}$), decreasing slightly at
 670 5 m, whereas during ebb tide nitrate concentrations decreased progressively from 20 to $10 \mu\text{mol L}^{-1}$ between 30
 671 and 10 m (Figure 6c). Nitrate concentrations in samples collected during the other sampling campaigns ranged
 672 from 12 to $32 \mu\text{mol L}^{-1}$, and appeared generally higher at stations visited during the September and November
 673 2020 campaigns compared to those in April and August 2021 (Figure S6).

674 Depth profiles collected in August 2021 revealed uniform nitrate $\delta^{15}\text{N}$ values of $\sim 7 \text{‰}$ at 30 m among
 675 profiles. In well-mixed profiles, nitrate $\delta^{15}\text{N}$ increased slightly to 7.5 ‰ above 10 m. In stratified profile, nitrate
 676 $\delta^{15}\text{N}$ increased progressively to 8.2 ‰ at 10 m (Figure 6d). Among all sampling campaigns, the $\delta^{15}\text{N}$ of nitrate
 677 ranged from 6.1 ‰ to 8.2 ‰, with median values of $6.8 \pm 0.4 \text{‰}$ (Figure 7a). The relationship between nitrate
 678 $\delta^{15}\text{N}$ and nitrate concentration in August 2021 was fit to a closed-system Rayleigh distillation model (Mariotti et
 679 al. 1981), suggesting a nitrate assimilation isotope effect of $1.5 \pm 0.1 \text{‰}$ (Figure 8).



680 **Figure 6.** Depth profiles during the August 2021 sampling campaign of (a) salinity, (b) temperature, (c) nitrate
 681 concentration, (d) the $\delta^{15}\text{N}$ of nitrate for analytical replicates and (e) the $\delta^{15}\text{N}$ of SPOM of replicate samples (n
 682 ≥ 2). Green and red symbols correspond to flood tide (collected between 11:00am and 2:00pm on August 2,
 683 2021), blue symbols correspond to ebb tide (collected at 9:00am on August 3, 2021).

680 The $\delta^{15}\text{N}$ of SPOM collected at depths above 35 m near Friday Harbor during the different sampling
 681 campaigns ranged from 1.6 to 11.7 ‰, averaging $5.7 \pm 1.7 \text{‰}$ (Figure 7b). Values were lowest for the four
 682 samples collected in April ($4.4 \pm 0.4 \text{‰}$), and highest for the four samples collected in September and November
 683 ($6.2 \pm 2.6 \text{‰}$), although these trends may be an artifact of the low data density in April ($n = 4$) and Sept./Nov. (n
 684 $= 5$) relative to August 2021 ($n = 29$), at which time the observed range of $\delta^{15}\text{N}$ subsumed that in the other two

Formatted: Font color: Text 1

Formatted: Font color: Text 1

Deleted: at 30 m

Formatted: Font color: Text 1

Formatted: Font color: Text 1

Deleted: ¶

Formatted: Font color: Text 1

Formatted: Line spacing: single

Formatted: Font color: Text 1

Formatted: Font color: Text 1

Deleted: spring

Deleted: autumn

Deleted: spring

Deleted: autumn

692 campaigns. Values did not differ coherently with depth in August 2021, although any potential depth structure
693 was obscured by the large variability among sample replicates (Figure 6e).

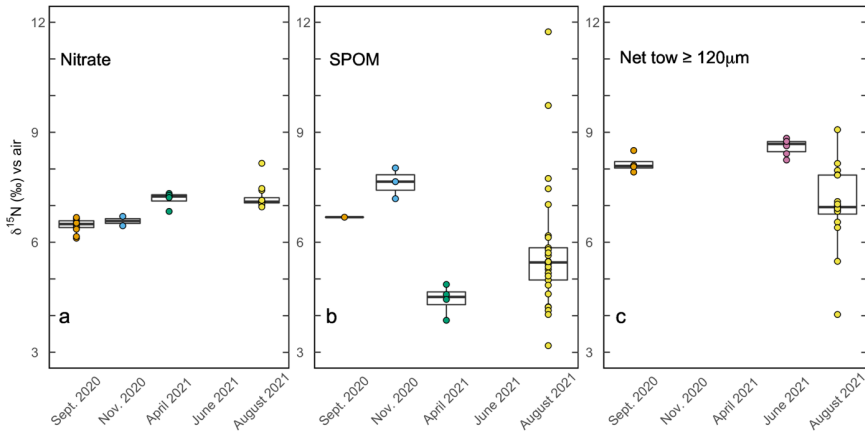


Figure 7. Boxplots of aqueous and particulate N pools at respective sampling times. (a) The $\delta^{15}\text{N}$ of nitrate from samples above 30 m collected during respective sampling campaigns. (b) The $\delta^{15}\text{N}$ of suspended particulate organic matter (SPOM) at sites near Friday Harbor during respective sampling campaigns. (c) The $\delta^{15}\text{N}$ of net tows ($\geq 120\ \mu\text{m}$ mesh size) conducted during respective sampling campaigns.

694 The $\delta^{15}\text{N}$ of material collected in net tows ($120\ \mu\text{m}$ mesh size) during sampling campaigns in September 2020,
695 and June 2021 ranged between 7.9 to 8.8 ‰ (Figure 7c). Material collected in net tows of $80\ \mu\text{m}$ and $150\ \mu\text{m}$
696 mesh size in August 2021 and separated by size class post-collection revealed a coherent $\delta^{15}\text{N}$ increase with size
697 class (Figure 7c; Figure 9). The $\geq 80\ \mu\text{m}$ size class had a mean $\delta^{15}\text{N}$ of $6.0 \pm 0.3\ \text{‰}$ whereas that $\geq 500\ \mu\text{m}$ had an
698 average $\delta^{15}\text{N}$ of $8.0 \pm 0.8\ \text{‰}$, which was significantly greater than the $\delta^{15}\text{N}$ of the other size classes (ANOVA, p-
699 value < 0.05).

700 4. Discussion

701 This study of *B. elegans* provides novel constraints on the trophic ecology of scleractinian CWCs. Foremost,
702 our observations of *B. elegans* collectively suggest that the relatively large global $\delta^{15}\text{N}$ offset of 8-9 ‰ between
703 CWC skeletal tissue and the $\delta^{15}\text{N}$ of PON exported from the surface ocean is neither explained by a large
704 difference between tissue and skeleton $\delta^{15}\text{N}$, nor by an unusually large trophic isotope effect. Further, controlled

Formatted: Font color: Text 1

Formatted: Font color: Text 1

Formatted: Font color: Text 1

Formatted: Font color: Text 1

Formatted: Line spacing: 1.5 lines

Formatted: Font color: Text 1

Formatted: Space Before: 10 pt, Line spacing: 1.5 lines

Formatted: Left, Indent: First line: 0.25", Space Before: 4 pt, After: 4 pt, Line spacing: 1.5 lines

705 feeding experiments yielded direct estimates of the trophic isotope effect and the corresponding N turnover **rate**
 706 of *B. elegans* soft tissue. Examination of soft tissue $\delta^{15}\text{N}$ of wild specimens in relation to regional hydrography
 707 and food web components near Friday Harbor **leads** us to conclude that *B. elegans* feeds predominantly metazoan
 708 zooplankton prey, implicating more than one trophic transfer between **exported** PON and coral soft tissue. We
 709 contextualize our findings to existing studies of CWC trophic ecology and discuss the implications of considering
 710 a two-level trophic transfer for paleo-reconstructions of ocean N cycling using *B. elegans* and CWCs **more**
 711 generally.

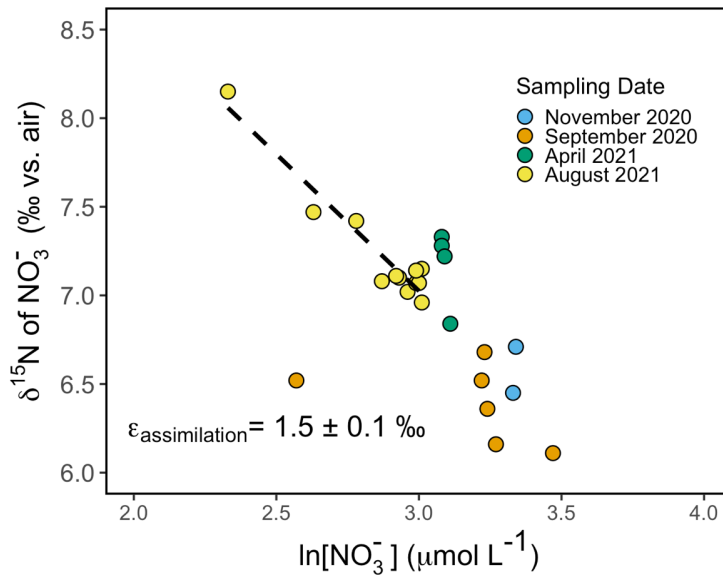


Figure 8. Rayleigh plot of nitrate $\delta^{15}\text{N}$ vs. \ln of nitrate concentration for samples collected from the surface to 40 m around Friday Harbor. The isotope effect of $\sim 1.5 \pm 0.1$ ‰ corresponds to the slope of the best fit linear regression line for the August 2021 data, $\delta^{15}\text{N}_{\text{NO}_3} = 11.7 - 1.5 \ln [\text{NO}_3^-]$.

4.1 Culture experiments revealed a normal trophic isotope effect

713 We **investigated** whether the large difference in $\delta^{15}\text{N}$ between PON export from the surface and coral
 714 skeleton-bound $\delta^{15}\text{N}$ (8-9 ‰) observed by Wang et al. (2014) could arise from an unusually large trophic level
 715 offset specific to CWCs. The long-term feeding experiment of *B. elegans* polyps revealed a ‘normal’ trophic

Deleted: time

Deleted: compels

Formatted: Font color: Text 1

Formatted: Font color: Text 1

Formatted: Font color: Text 1

Formatted: Font color: Text 1

Formatted: Font: 11 pt, Font color: Text 1

Formatted: Font: 11 pt, Font color: Text 1

Formatted: Font: 11 pt, Font color: Text 1

Formatted: Font: 11 pt, Font color: Text 1

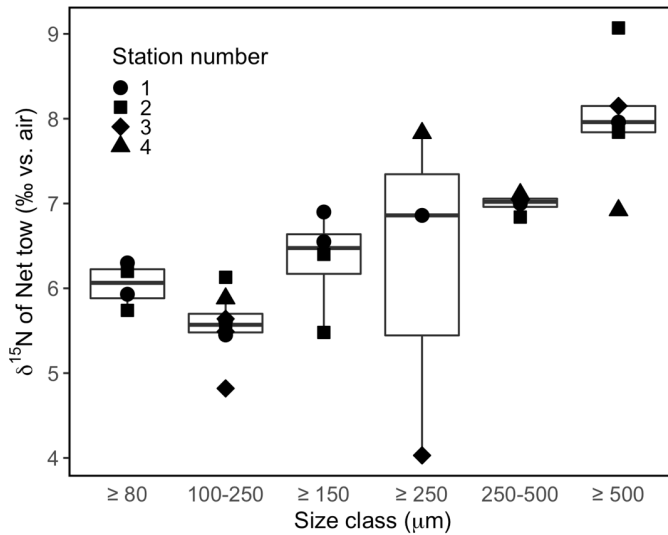
Formatted: Font: 11 pt, Font color: Text 1

Deleted: queried

Formatted: Font color: Text 1

Formatted: Font color: Text 1

719 isotopic offset between coral tissue and diet of $\epsilon = +3.0 \pm 0.1 \text{ ‰}$. This value conforms to the expected range of
 720 $+3.4 \pm 1.1 \text{ ‰}$ for a single trophic level offset in $\delta^{15}\text{N}$ (Minagawa and Wada, 1984).



Deleted: (
 Deleted: of
 Deleted: - a value that
 Deleted:)

722 Figure 9. Boxplots of net tow material collected above 30 m in August 2021, separated by size class.

723 To support the above conclusion, we assess the assumptions inherent to the isotope mixing model (Eq. 1)
 724 used to derive ϵ and the corresponding nitrogen turnover rate from our culture data. First, the model only
 725 accounts for the turnover of a single pool of N, requiring the assumption that all N in the coral polyp tissues
 726 equilibrate at the same rate. This notion is unlikely to be wholly accurate, as fluxes of N may vary among tissue
 727 types. However, given the relatively low resolution of our sampling over the course of the culture experiments
 728 (necessary due to constraints on numbers of total samples) we are unable to extend our model to one with
 729 multiple pools (e.g. as in Ayliffe et al. 2004). As soft tissues of individual coral polyps were homogenized, we
 730 suggest that the $\delta^{15}\text{N}$ values and corresponding estimate of ϵ thus represent the average of soft tissues with
 731 potentially different turnover rates. The estimates of ϵ and N turnover rate further rely on the assumption that the

Formatted: Font color: Text 1
 Formatted: Line spacing: single
 Formatted: Font color: Text 1
 Formatted: Font color: Text 1
 Formatted: Line spacing: 1.5 lines
 Deleted: turnover
 Deleted: turnover time
 Deleted: ies
 Formatted: Font color: Text 1
 Deleted: s
 Formatted: Font color: Text 1

740 nutritional quality of the respective diets among treatments was equivalent, as trophic isotope effects can be
741 sensitive to food type. Diets low in protein can be associated with greater ϵ values due to internal recycling of
742 nitrogen (Adams and Sterner, 2000; Webb et al., 1998). For instance, locusts fed a low protein diet were enriched
743 5.1 ‰ from their diet, compared to 2.3‰ for those fed a high protein diet (Webb et al., 1998). Conversely, a
744 compilation of studies of various metazoan consumers raised on controlled diets suggests that high protein diets
745 generally result in higher trophic isotope effects (~3.3 ‰) compared to more herbivorous diets (~2.2 ‰), a
746 dynamic ascribed to higher rates of N excretion to assimilation in consumers fed high protein diets (McCutchan
747 Jr et al., 2003). ~~As noted in Table S3 and in Section 2.3.1, our *Artemia* prey had similar C:N ratios among~~
748 ~~treatments, in line with our model treatment. Finally, our model assumes that N turnover was dominated by~~
749 ~~metabolic tissue replacement, rather than net growth, consistent with the observation that adult *B. elegans* growth~~
750 ~~is slow (Gerrodette 1981).~~

751 Equation 1 could be invalidated ~~if the corals can access nutritional N sources other than N in *Artemia*, given~~
752 ~~that the model assumes that *Artemia* are the only source of N to corals in our experiment.~~ Biological N₂ fixation
753 and chemoautotrophy have been detected in association with CWC holobionts, providing some N nutrition to the
754 corals (Middelburg et al., 2016). Our trophic isotope effect estimate was in the range expected for a single trophic
755 transfer, arguably suggesting that N₂ fixation, if occurring, ~~was not a substantial contribution~~ to the corals'
756 nutrition; it would otherwise result in a lower value of ϵ given a $\delta^{15}\text{N}$ contribution of -1 to 0 ‰ (Carpenter et al.
757 1997). That the trophic isotope effect of the poorly fed corals did not differ from that of corals that were well-fed
758 also argues for no sources of N additional to the *Artemia*, as starved corals would presumably increase their
759 reliance on said source. In a related vein, N recycling between the *B. elegans* specimens and potential microbial
760 symbionts (e.g. Middelburg et al. 2016) could also dampen the trophic isotope effect relative to the *Artemia* prey
761 and yield an over-estimate of soft tissue ~~turnover rate for N~~. The normal trophic isotope effect ~~indicated here~~
762 ~~suggests~~ a modest role of N retention and recycling by microbial symbionts, in contrast to tropical symbiotic
763 corals wherein bacterial symbionts promote substantial N retention and recycling, and consequently lower trophic
764 isotope effects (Tanaka et al. 2018). Finally, the validity of our estimates could be sensitive to differences in
765 feeding rates, which can influence the rate of N turnover of tissues (Martinez del Rio and Carleton, 2012; Rangel
766 et al., 2019). Corals were fed at identical times among treatments, at a relatively high feeding rate (Crook et al.,
767 2013). However, given the limited number of studies on feeding in *B. elegans*, it is difficult to compare our
768 feeding strategy and that of this species' natural environment. Overall, we consider that the mixing model

Deleted: To avoid diet quality confounding our estimates, we verified that the...

Deleted: ensuring a similar nutritional value

Deleted: The end-member mixing represented by

Deleted: also

Deleted: given

Deleted: additional to

Deleted: the

Deleted: s

Deleted: contributed modestly

Deleted: 2016)

Formatted: Not Highlight

Deleted: turnover

Deleted: evinced

Deleted: argues for

Deleted: to encourage growth

784 described by Equation 1 is appropriate to derive the first-order trophic isotope effect and turnover rate of *B.*
785 *elegans*.

786 Changes in metabolism due to underfeeding or prolonged fasting have the potential to increase trophic-level
787 isotope offsets due to increased protein metabolism (Adams and Sterner, 2000). For instance, extensive amino
788 acid recycling in overwintered adult insect larvae was cited to explain trophic isotope effects upward of 10‰
789 (Scrimgeour et al., 1995). A meta-analysis on the effects of starvation on consumer $\delta^{15}\text{N}$ revealed that starvation
790 generally led to increased organism $\delta^{15}\text{N}$ by an average of 0.5 ‰, up to 4.3 ‰ (Doi et al., 2017). This dynamic
791 was documented for the tropical symbiotic coral *Stylophora phistillata*, where heterotrophically starved corals
792 were enriched in $\delta^{15}\text{N}$ by ~0.5 ‰ compared to frequently fed corals (Reynaud et al., 2009). The trophic isotope
793 offset of *B. elegans* soft tissue relative to its diet, ϵ , was not discernibly influenced by near starvation; that of
794 corals fed once every other week was similar to that of corals fed twice a week – in spite of visible signs of stress
795 among the former, including relatively more sluggish feeding (Figure S7) and thinner soft tissue (data not
796 shown). Deep sea coral reefs are often highly productive environments with high levels of biodiversity,
797 commensurate with a relatively high food supply (Duineveld et al., 2007; 2004; Genin et al., 1986; Roberts et al.,
798 2006; Soetaert et al., 2016; Thiem et al., 2006; Cathalot et al. 2015). Nevertheless, periodicity and spatial
799 heterogeneity in the food supply of CWC reefs implicate periods of lower food density (e.g., Duineveld et al.
800 2007). High currents, downwelling and/or vertically migrating zooplankton temporally boost the export of
801 surface organic matter to the seabed, creating ‘feast’ conditions, interspersed with ‘famine’ periods during the
802 non-productive season (Maier et al. 2023). Regardless, our trials suggest that starvation, if pertinent to CWC
803 communities, does not result in greater-than-expected trophic isotope offsets, at least for *B. elegans*.

804 4.2 Turnover rate for *B. elegans*

805 We report the first estimate of the nitrogen turnover for a non-symbiotic cold-water coral of 291 ± 15 days
806 for *B. elegans* soft tissue. This value falls within the range of existing estimates for tropical symbiotic corals.
807 Pulse-chase experiments with ^{15}N -nitrate conducted with fragments of the tropical symbiotic coral *Porites*
808 *cylindrica* yielded a N turnover time of 370 days, and of 210 days for the tropical symbiotic coral *Acropora*
809 *pulchra* (Tanaka et al. 2006; 2018). These relatively long turnover times are attributed to the recycling and
810 retention of N within the coral-symbiont system in nutrient-deplete ecosystems. In comparison, the corresponding
811 carbon turnover in *A. pulchra* was 18 days – compared to 210 days for N – because the system is ultimately N
812 limited (Tanaka et al., 2006). Tanaka et al. (2018) inferred that the N turnover in *P. cylindrica* would be
813 substantially faster than 370 days without symbionts, on the order of 56 days based on estimates of polyp-specific

Deleted: time

Deleted: The extent to which CWCs experience significant periods of starvation *in-situ* is unclear.

Formatted: Font color: Text 1

Formatted: Font color: Text 1

Formatted: Font color: Text 1

Deleted: ; Kiriakoulakis et al. 2007

Deleted: time

Deleted: of

Formatted: Font: Italic

Formatted: Font color: Text 1

820 N uptake rates. Nevertheless, the N turnover estimated for the tropical symbiotic coral *Porites lutea* was notably
821 shorter than *A. pulchra* and *P. cylindrica*, on the order of 87 days (Rangel et al., 2019), implicating different N
822 nutritional strategies among symbiotic coral groups and/or ecosystems. The N turnover for *B. elegans* estimated
823 here is of the same order ~~as but still longer than~~ that for tropical symbiotic corals suggesting that cold-water
824 species have lower ~~metabolic and~~ growth rates compared to tropical symbiotic species, although efficient N
825 recycling has also been documented previously in cold-water corals (Middelburg et al. 2016). The slower
826 turnover of CWCs relative to their symbiotic tropical counterparts may reflect the lower temperatures of the
827 former's habitats (Miller, 1995; Thomas and Crowther 2015).

828 Constraints on N turnover also allow for calibration of the temporal resolution that is achievable with the
829 CWCs $\delta^{15}\text{N}$ proxy for marine N cycling. Corals are constantly accreting skeleton, such that coral proxies have the
830 potential to provide annual resolution (*e.g.*, Adkins et al. 2004). In theory, a rapid N turnover in CWC could
831 record seasonal changes in regional N dynamics. A turnover time of 291 ± 15 days for N in *B. elegans* soft tissue,
832 however, signifies that the $\delta^{15}\text{N}$ of coral skeleton is unlikely to provide a faithful record of seasonal differences in
833 the $\delta^{15}\text{N}$ of the coral diet. Moreover, the turnover of the pool of N that sources the skeletal tissue may be different
834 from that of bulk tissue, and thus decoupled from the soft tissue turnover ~~rate~~. We suggest that CWCs can likely
835 record changes in their diet on annual or longer timescales, compatible with the ability to date CWC with
836 subdecadal resolution (Adkins et al. 2004).

837 4.3 Soft tissue vs. skeleton $\delta^{15}\text{N}$

838 A large biosynthetic $\delta^{15}\text{N}$ offset between the coral soft tissue and its skeleton could conceivably account for a
839 large $\delta^{15}\text{N}$ offset between coral skeleton-bound organic matter and N of export that is not explained by single
840 trophic level enrichment of $\sim 3\%$. However, the mean difference between soft tissue and skeleton-bound $\delta^{15}\text{N}$
841 among *B. elegans* specimens collected at Friday Harbor was relatively modest, on the order of $+1.2\%$, ranging
842 between $+0.5$ and $+2.2\%$. The observed range was dictated primarily by the variability in the $\delta^{15}\text{N}$ of the coral
843 soft tissue, as skeleton-associated $\delta^{15}\text{N}$ values were relatively invariant among specimens sampled from different
844 locations and field seasons ~~likely due to the fact that the amount of skeleton analyzed represented multiple~~
845 years of growth. The amount of skeleton-bound organic N is small relative to aragonite mass ($2\text{-}5\ \mu\text{mol N per g}$
846 of skeleton in our samples), such that homogenization of 50-100 mg aragonite fragments may alias seasonally-
847 driven variability in skeletal $\delta^{15}\text{N}$. Soft tissue values in spring were $\sim 1.5\%$ higher than in summer and fall, such
848 that they appeared to record seasonal changes in diet (Figure 5a). In this regard, the asymptotic nature of the two
849 end-member isotope mixing model (Eq. 1) renders *B. elegans*'s soft tissue sensitive to seasonal changes in prey

Deleted: as

Deleted: and/or metabolisms

Deleted:

Formatted: Font: Italic, Font color: Text 1

Formatted: Font color: Text 1

Deleted: time

Formatted: Font color: Text 1

Deleted: ,

Deleted: worth

Formatted: Font color: Text 1

Formatted: Font color: Text 1

Formatted: Font color: Text 1

856 $\delta^{15}\text{N}$, but not likely to reach isotopic equilibrium on seasonal timescales - given an N turnover of ~291 days, as
857 discussed above. Seasonal variations in the $\delta^{15}\text{N}$ of the food source of *B. elegans* near Friday Harbor could arise
858 from corresponding differences in the $\delta^{15}\text{N}$ of nitrate entrained to the surface driven by seasonal hydrographic
859 variability around San Juan archipelago, in the extent of surface nitrate consumption, in food web structure, or
860 from some combination of these. The data density among all but the August 2021 sampling campaign is too
861 sparse to be conclusive in this regard. Otherwise, the observed differences in soft tissue $\delta^{15}\text{N}$ may result from
862 spatial heterogeneity in food source $\delta^{15}\text{N}$ among the different collection sites visited for respective campaigns at
863 Friday Harbor.

Formatted: Font color: Text 1

864 As documented here for *B. elegans*, the $\delta^{15}\text{N}$ difference between coral tissue and skeleton appears to be
865 modest among various scleractinian coral species. Specimens of the symbiotic tropical coral *Porites lutea* showed
866 a $\delta^{15}\text{N}$ offset of +1.1 ‰ between skeleton and soft tissue, whereas the symbiotic tropical coral *Favia stelligera*
867 revealed an insignificant offset of -0.1 ‰ (Erlor et al., 2015). Similarly, no offset was observed for proteinaceous
868 cold-water corals of the genus *Lepidisis* collected off Tasmania (Sherwood et al., 2009), whereas an offset of -1.9
869 \pm 0.8 ‰, was reported for cold-water proteinaceous corals of the genus *Primnoa* from the Gulf of Alaska,
870 *Isadella* from the Central California Margin, and *Kulamanamana* from the North Pacific Subtropical Gyre
871 (McMahon et al., 2018). Conversely, a study of numerous species of both symbiotic and non-symbiotic corals
872 reported a +4 ‰ offset between the skeletal organic matrix and soft tissue among the non-symbiotic corals
873 specifically, but no difference among the symbiotic corals (Muscatine et al., 2005), suggesting that biosynthetic
874 offsets may occur for certain CWC species or conditions.

875 4.4 Implications for components of CWC diet

876 Cold water corals are considered opportunistic feeders, ingesting whatever is available in the water column
877 (Mortensen, 2001; Freiwald, 2002; Duineveld et al. 2004; 2007; Kiriakoulakis et al. 2005; Carlier et al. 2009;
878 Dodds et al. 2009; van Oevelen et al. 2009). They are reported to feed on zooplankton (Kiriakoulakis et al., 2005;
879 Naumann et al., 2011), including microzooplankton (Houlbrèque et al. 2004), on phytoplankton and
880 phytodetritus, including the bacterial fraction of phytodetritus (Maier et al., 2020; Houlbrèque et al. 2004),
881 dissolved organic matter (Mueller et al., 2014; Ferrier 1991; Al-Moghrabi et al. 1993; Hoegh-Guldberg &
882 Williamson 1999; Houlbrèque et al. 2004; Grover et al. 2008), and the CWC holobiont has been observed to
883 display biological N_2 fixation and chemoautotrophy (Middelburg et al. 2016). While it is clear that corals may be
884 able to consume a variety of components within the food web, the soft tissue $\delta^{15}\text{N}$ of *B. elegans* specimens
885 collected at Friday Harbor averaged 12.0 ‰, signifying that they fed on material with a $\delta^{15}\text{N}$ of approximately

Deleted: C

Deleted: g

Formatted: Font color: Text 1

Formatted: Indent: First line: 0", Line spacing: 1.5 lines

Deleted: 2012.

Deleted: v

Formatted: Not Highlight

Formatted: No underline, Font color: Text 1

Formatted: Font color: Text 1

Formatted: No underline, Font color: Text 1

Formatted: Font color: Text 1

Formatted: No underline, Font color: Text 1

Formatted: Font color: Text 1

Formatted: No underline, Font color: Text 1

Formatted: Font color: Text 1

Moved (insertion) [3]

890 9.0 ‰ – accounting for a normal trophic offset relative to their diet (3 ‰) confirmed by our culture experiment
 891 results. Here, we seek to determine the primary nutrition source for *B. elegans* at Friday Harbor by comparing the
 892 $\delta^{15}\text{N}$ of these corals' expected diet with measured $\delta^{15}\text{N}$ of different food web components including SPOM and
 893 net tow material.

894 We first explore whether the SPOM fraction of the food web was the dominant component of *B. elegans*' diet
 895 at Friday Harbor. SPOM is operationally defined as the particulate material retained onto glass fiber filters (GF/F,
 896 0.7 μm nominal pore size) from filtered aqueous samples. At the ocean surface, including at the stations near
 897 Friday Harbor, SPOM is generally dominated by phytoplankton material. At the ocean subsurface, below the
 898 euphotic zone, SPOM derives from organic material exiting the ocean surface, but is considered a distinct pool
 899 from the ballasted sinking PON collected in sediment traps. The $\delta^{15}\text{N}$ of SPOM typically increases with depth,
 900 with the steepest gradient across the 100-300 m depth interval, reaching upwards of ~4-5 ‰ in the ocean
 901 subsurface, which are higher values than the corresponding sinking particles at abyssal depths due to recycling
 902 and remineralization (Altabet, 1988; Casciotti et al., 2008; Saino and Hattori, 1987). Wang et al. (2014) reasoned
 903 that because the $\delta^{15}\text{N}$ of SPOM is approximately one trophic level lower than that of the N preserved in skeletons of
 904 the deep-dwelling (deeper than ~500 m) CWC *Desmophyllum dianthus*, and because suspended particles are the
 905 most abundant form of small particles in the deep ocean, cold-water corals must feed predominantly on SPOM.
 906 However, SPOM collected in the upper 30 meters near Friday Harbor was 5.7 ± 1.7 ‰, which is ~6 ‰ lower
 907 than *B. elegans* soft tissue, a difference greater than expected for a single trophic level. Thus, the SPOM at Friday
 908 Harbor was evidently not the predominant food source for *B. elegans* growing in this depth interval.

909 Additionally, it has been suggested that CWCs can assimilate dissolved organic nitrogen (DON) (Gori et al.,
 910 2014). We do not have $\delta^{15}\text{N}$ DON measurements from our field study. However, we do not expect the potential
 911 assimilation of DON to explain the elevated $\delta^{15}\text{N}$ of organic tissue that was observed. There are two components
 912 of marine DON, refractory and labile (Bronk et al. 2002), which have different $\delta^{15}\text{N}$ (Knapp et al. 2018). At
 913 Friday Harbor, we don't know the partitioning of the $\delta^{15}\text{N}$ between these pools, but even if we did, the labile
 914 fraction (which would presumably be the pool available to corals) is expected to converge on the $\delta^{15}\text{N}$ value of
 915 SPOM (Bronk et al., 2002, Sigman and Fripiat 2019 their Fig. 4; Knapp et al., 2018, Zhang et al., 2020), given
 916 that the most recently produced DON is generally most labile. As a result, consumption of DON would not
 917 explain the high $\delta^{15}\text{N}$ of coral organic tissue.

918 Instead, we suggest that the relatively high $\delta^{15}\text{N}$ of ~12 ‰ of *B. elegans* soft tissue at Friday Harbor results
 919 from these corals deriving nutrition predominantly from larger metazoan zooplankton. Indeed, this is supported
 920 by a comparison of the $\delta^{15}\text{N}$ coral tissue and the $\delta^{15}\text{N}$ of the largest size class of net tow material ($\geq 500 \mu\text{m}$) of

- Deleted: incubation
- Deleted: .
- Moved up [3]: soft tissue $\delta^{15}\text{N}$ of *B. elegans* specimens collected at Friday Harbor averaged 12.0 ‰, signifying that they fed on material with a $\delta^{15}\text{N}$ of approximately 9.0 ‰ – accounting for a normal trophic offset relative to their diet (3 ‰).
- Deleted: ¶
- There is a lack of consensus, however, regarding which components of the food web dominate their diets. The
- Formatted: Font color: Text 1
- Deleted: defined as
- Deleted:
- Deleted:
- Deleted: in the ocean subsurface
- Deleted: can be
- Deleted: heavier
- Formatted: Font color: Text 1
- Formatted: Font color: Text 1
- Deleted:
- Formatted: Font color: Text 1
- Deleted: *D. dianthus*
- Formatted: Font color: Text 1
- Deleted: X ‰ (JOSIE, CAN YOU PLEASE, PROVIDE THE ACTUAL VALUE HERE
- Deleted:), WHICH IS
- Formatted: Not Highlight
- Deleted: T
- Formatted: Font color: Text 1
- Formatted: (... [17])
- Formatted: Font: 11 pt, Font color: Text 1
- Deleted: A more parsimonious explanation to account for the
- Formatted: Font color: Text 1
- Formatted: Font color: Text 1
- Formatted: Font color: Text 1
- Formatted: Line spacing: 1.5 lines
- Deleted: is that they derived
- Formatted: Font color: Text 1
- Deleted: A direct positive relationship between
- Deleted:
- Deleted: of material collected in net tows and particle size (... [18])
- Formatted: Font color: Text 1

949 $8.0 \pm 0.8 \%$. This is the only component of the organic matter nitrogen budget that is offset from the coral tissue
950 by $\sim 3.5 \%$, consistent with one trophic level transfer. Additionally, the net tow material had a molar C:N ratio of
951 4.4 ± 0.6 , compared to 6.5 ± 2.2 for the SPOM (Figure S8), suggesting a dietary preference for metazoan
952 zooplankton would provide higher protein content and nutritional density for these corals (Adams and Sterner,
953 2000).

954 Despite evidence for zooplankton as the main dietary source for *B. elegans* at Friday Harbor, we
955 acknowledge that this feeding strategy may not apply for corals of other species living in habitats that are
956 hundreds to thousands of meters deep. As pointed out in a recent review (Maier et al. 2023), the presence of
957 CWC reefs in the food-limited deep ocean appears paradoxical, and it is not likely that the food available to
958 corals at Friday Harbor looks identical to food available to corals living at >1000 m water depth. Indeed, Maier et
959 al. 2023 suggest that the biodiversity and productivity of CWC reefs in the deep sea are supported by a number of
960 processes such as CWC's ability to consume a range of dietary components (DOM, bacterioplankton, inorganic
961 resources such and inorganic C and ammonium), efficient resource recycling, and their ability to align their
962 feeding strategies and growth with fluctuations in food availability.

963 Maier et al. (2023) and references therein highlight that most deep CWC reefs occur in regions with higher-
964 than-average annual primary productivity, indicating that these CWC reefs are sustained by inputs of high energy
965 to the system, where there is also evidence for the presence of vertically migrating zooplankton. The vertically
966 migrating zooplankton have been found near both relatively shallow (<200 m, Duineveld et al. 2007, Garcia-
967 Herrera et al., 2022) and deep (~ 1000 m, e.g. Carlier et al. 2009) CWC reefs. Moreover, there are a number of
968 other independent studies that reveal a single trophic level offset between the $\delta^{15}\text{N}$ of zooplankton prey and the
969 $\delta^{15}\text{N}$ soft tissue of asymbiotic scleractinian corals at specific sites (Duineveld et al., 2004, Sherwood et al. 2005;
970 2008; 2009; Carlier et al., 2009; Hill et al., 2014; Maier et al., 2020). Given the 'normal' trophic level offset
971 reported for CWCs in our laboratory culture experiment, these published observations underscore that
972 zooplankton could be a dominant dietary component of corals other than *B. elegans* as well. Additional evidence
973 from lipid biomarkers corroborates the assertion that deep-dwelling CWC species such *Lophelia pertusa*
974 (recently re-classified as *Desmophyllum pertusum*) and *Madrepora oculata* feed predominantly on metazoan
975 zooplankton (Dodds et al., 2009; Kiriakoulakis et al., 2005; Naumann et al. 2015). Some deep-dwelling CWCs
976 (*Desmophyllum pertusum*, *Madrepora oculata*, *Dendrophyllia cornigera*) exhibit prey preference for larger
977 zooplankton (Da Ros et al. 2022), suggesting that zooplankton prey are an essential component of their diet.
978 Indeed, an exclusive diet of phytodetritus (Maier et al. 2019) and the exclusion of zooplankton from diet

Deleted: X‰ (JOSIE, CAN YOU PLEASE, PROVIDE THE ACTUAL VALUE HERE as well)

Deleted: clearly shows an offset consistent with one trophic transfer, whose $\delta^{15}\text{N}$ was ($\sim 3.5 \%$) lower than coral soft tissue – approximating a single trophic transfer.

Deleted: OM

Deleted: At Friday Harbor

Formatted: Font color: Text 1

Deleted: support

Deleted: in the former

Formatted: Font color: Text 1

Formatted: Font color: Text 1

Deleted: in

Deleted: ,

Formatted: Font color: Text 1

Formatted: Font color: Text 1

Formatted: Font color: Text 1

Deleted: activity

Deleted: Nevertheless,

Formatted: Font: Italic

Deleted: s

(Naumann et al. 2011) led to decreases in coral metabolism. More fundamentally, the shared traits of tentacles and nematocysts are evidence of a predatory life strategy, indicating that zooplankton are an important food source for corals (Lewis and Price, 1975; Sebens et al., 1996). The coral morphology of *B. elegans* and that of other cold water scleractinian corals is consistent with an adaptation for the capture of prey of a commensurate size (Fautin, 2009). Correspondingly, *D. dianthus* is considered to be a generalized zooplankton predator that can prey on medium to large copepods and euphasiids (Höfer et al., 2018). In contrast, gorgonian corals do not capture naturally occurring zooplankton and have a correspondingly low density of nematocysts (Lasker 1981). In summary, while our data cannot directly indicate that all CWCs, including the deep-dwelling ones, derive their primary nutrition from zooplankton, the results of our trophic experiment and field study (when evaluated in the context of the published literature) suggest that it may be important to consider metazooplankton as a significant component of CWC diet, and that CWC $\delta^{15}\text{N}$ is likely to be sensitive to food web dynamics. We discuss the implications of these suggestions further in the sections below.

4.5 Does coral-bound $\delta^{15}\text{N}$ reflect surface ocean processes at Friday Harbor?

The effectiveness of coral skeleton-bound $\delta^{15}\text{N}$ as an archive to reconstruct past ocean N cycling depends on its ability to record the $\delta^{15}\text{N}$ of the surface PON export. In turn, the $\delta^{15}\text{N}$ imparted to the phytoplankton component of surface particles, from which PON export derives, is highly dependent on surface ocean dynamics that influence the degree of nitrate consumption and associated isotope fractionation. Here, we describe local marine N cycling dynamics in order to evaluate whether coral-bound $\delta^{15}\text{N}$ recorded in the *B. elegans* specimens reflects local surface ocean processes.

Given complete assimilation of inorganic N pools, the $\delta^{15}\text{N}$ of phytoplankton material - the dominant component of SPOM at the surface ocean - converges on the $\delta^{15}\text{N}$ of the N sources, new nitrate and recycled N sources (Treibergs et al., 2014; Fawcett et al. 2011). At steady state, the $\delta^{15}\text{N}$ of the sinking PON flux reflects the isotope signature of the nitrate upwelled to the surface (Altabet, 1988). Alternatively, given partial nitrate consumption in the context of a finite pool (Rayleigh dynamic), such as in high-nutrient low-chlorophyll regions and in upwelling systems, the SPOM $\delta^{15}\text{N}$ is fractionated relative to the nitrate $\delta^{15}\text{N}$ as function of the assimilation isotope effect and the extent of nitrate consumption (Sigman et al., 1999). The $\delta^{15}\text{N}$ of the sinking flux then reflects both the $\delta^{15}\text{N}$ of nitrate upwelled to the surface and the degree of nitrate consumption (Altabet and François 1994; François et al. 1997). In this section, we discuss whether coral-bound $\delta^{15}\text{N}$ reflects the $\delta^{15}\text{N}$ of nitrate entrained to the surface.

Deleted: possible

Deleted: primary

Deleted: ies may differ among asymbiotic coral species and that CWCs may obtain nutrients from a wide range of sources when necessary. For instance, N and C isotope ratios among gorgonian soft coral species collected off the coast of Newfoundland suggest that some feed predominantly on fresh phytodetritus, while others rely on microplankton and thus display higher trophic levels (Sherwood et al., 2008). Additionally, some asymbiotic corals may produce mucus nets to capture suspended particles, whereby corals disperse mucus filaments with their mouth and tentacles and the particles entrapped by the mucus are then drawn back into the mouth for feeding (Lewis and Price, 1975). We observed mucus production by *B. elegans* only when polyps were out of water – a behavior ascribed to the mitigation of desiccation (Brown and Bythell, 2005); .measurements the potential assimilation of wasmarine , (Bronk et al. 2002) (Knapp et al. 2018),..generally*

The assertion that metazoan zooplankton are the dominant dietary component of scleractinian CWCs – despite their ability to be omnivorous – is indeed supported by a number of independent studies. The single trophic level between the $\delta^{15}\text{N}$ of zooplankton prey and the soft tissue of many asymbiotic corals has generally been interpreted to indicate that zooplankton are the dominant component of their diet (Duineveld et al., 2004; Sherwood et al. 2005; 2008; 2009; Carrier et al., 2009; Hill et al., 2014; Maier et al., 2020). Additional evidence from lipid biomarkers corroborates the assertion that deep-dwelling CWC species such *Lophelia pertusa* and *Madrepora oculata* feed predominantly on metazoan zooplankton (Dodds et al., 2009; Kiriakoulakis et al., 2005; Naumann et al. 2015). Deep-dwelling CWCs (*Desmophyllum pertusum*, *Madrepora oculata*, *Dendrophyllia cornigera*) also exhibit prey preference for larger zooplankton (Da Ros et al. 2022), suggesting that zooplankton prey are an essential component of their diet. Indeed, an exclusive diet of phytodetritus did not satisfy the fatty acid requirements of *Lophelia pertusa*, requiring supplementation with metazoan zooplankton to achieve maximum growth (Maier et al., 2019). Similarly, zooplankton exclusion from the diet of the solitary CWC *D. dianthus* resulted in a decrease in coral respiration (Naumann et al. 2011). More fundamentally, the shared traits of tentacles and nematocysts are evidence of a predatory life strategy, indicating that zooplankton are an important food source for corals (Lewis and Price, 1975; Sebens et al., 1996). The coral morphology of *B. elegans* and that of other cold water scleractinian corals is consistent with an adaptation for the capture of prey of a commensurate size (Fautin, 2009). Correspondingly, *D. dianthus* is considered to be a generalized zooplankton pred (... [19])

Formatted: Font color: Text 1

Deleted: faithfulness

Deleted: its

Deleted: to

Formatted: No underline, Font color: Text 1

Formatted: Font: Italic, No underline, Font color: Text 1

Formatted: No underline, Font color: Text 1

Formatted: Font color: Text 1

Deleted: HNLC

Deleted:

1143 Nitrate assimilation at Friday Harbor ~~appeared to be~~ incomplete, potentially implicating the fractionation of
1144 N isotopes between nitrate and biomass. Although ~~depleted~~ nitrate concentrations are generally expected at
1145 coastal sites during the summer ~~in density stratified water column~~ due to phytoplankton assimilation, nitrate
1146 concentrations at Friday Harbor in August of 2021 were upwards of 15 μM at the surface and 20 μM at 30 m
1147 depth. Indeed, nitrate in the San Juan Channel is replete year-round, even at the surface, due to vigorous mixing
1148 within the channel (Mackas and Harrison, 1997; Murray et al., 2015).

1149 The region experiences tidal mixing, designating ~~it as~~ a well-mixed estuary with minimal ~~density~~
1150 ~~stratification~~ (Banas et al., 1999; Mackas and Harrison, 1997). ~~The tidal influence is clearly identified from the~~
1151 ~~diurnal patterns of vertical hydrographic structure variability with the salinity/temperature gradients changing~~
1152 ~~with the tidal phase (Figure 6a and b). The tidal pumping drives vertical mixing between~~ high nutrient deep water
1153 from the Juan de Fuca Strait and fresher surface water from the Strait of Georgia (Banas et al., 1999; Lewis,
1154 1978; Murray et al., 2015; Mackas and Harrison, 1997). Nutrient concentrations in the surface Georgia Strait vary
1155 seasonally and are depleted during the summer at the stratified, fresher surface (Del Bel Belluz et al., 2021;
1156 Mackas and Harrison, 1997). ~~Our temperature-salinity plot in August 2021 reflects~~ end-member mixing ~~between~~
1157 more saline/colder water from the Juan de Fuca Strait with fresher/warmer surface water from the Georgia Strait
1158 (Figure S9; Banas et al., 1999). The influence of Georgia Strait surface water is recognized by the salinity
1159 minima originating from the outflow of the Fraser River (Figures S10; Mackas and Harrison, 1997). ~~The nitrate~~
1160 ~~profiles in August 2021, though collected with a lower vertical resolution, do show diurnal variability in vertical~~
1161 ~~gradients similar to salinity/temperature, consistent with the tidal mixing effect (Figure 6c).~~

1162 The $\delta^{15}\text{N}$ of nitrate measured at stations near Friday Harbor ~~also~~ corroborate the mixing of nitrate-rich deeper
1163 water with nitrate-deplete surface water from Georgia Strait. The apparent isotope effect for nitrate assimilation
1164 in August 2021 was $\sim 1.5\%$, markedly lower than the canonical value of 5% associated with nitrate assimilation
1165 by surface ocean phytoplankton communities (DiFiore et al., 2006; Sigman et al., 1999; Altabet and François,
1166 1994). A low apparent isotope effect is consistent with ~~two~~ end-member mixing of lower $\delta^{15}\text{N}$, nitrate-rich water
1167 with highly fractionated (high $\delta^{15}\text{N}$), low-nitrate water (Sigman et al., 1999). Highly fractionated nitrate, in turn,
1168 likely originated from ~~nutrient-depleted~~ Georgia Strait surface waters entrained into the Channel Islands. The
1169 linear relationship between salinity and nitrate concentration in August 2021 further ~~substantiates~~ physical
1170 mixing as the dominant control on nitrate concentrations and isotope ratios in San Juan Channel (Figure S10;
1171 Mackas and Harrison, 1997). Moreover, the $\delta^{15}\text{N}$ of nitrate was relatively uniform with depth, indicating effective
1172 ~~vertical mixing of the Georgia Strait and Juan de Fuca Strait water masses~~. The relatively slight decrease in

Deleted: was ostensibly

Deleted: low surface

Formatted: Font color: Text 1

Deleted: Juan de Fuca Strait as

Deleted: vertical density

Formatted: Font color: Text 1

Deleted: gradients

Deleted: Nutrients are supplied to the broader region by upwelling (Lewis, 1978; Murray et al., 2015; Mackas and Harrison, 1997).

Deleted: The water in the San Juanthis region Channel comprises a mix of ...

Deleted: .

Deleted: , in turn,

Deleted: The

Deleted: s

Deleted: (Figure 6a,b)

Deleted: corroborate

Deleted: of

Formatted: Font color: Text 1

Deleted: and

Deleted: and

Formatted: Font color: Text 1

Formatted: Font color: Text 1

Formatted: Font color: Text 1

Formatted: Font color: Text 1

Deleted: (assimilated)

Formatted: Font color: Text 1

Formatted: Font color: Text 1

Deleted: corroborates

1193 nitrate $\delta^{15}\text{N}$ with depth suggests a secondary influence of local nitrate assimilation on its concentration and
1194 isotope ratios.

1195 The corresponding $\delta^{15}\text{N}$ of SPOM at Friday Harbor covered a broad range, from 4.2 ‰ to 8.7 ‰ in August
1196 2021. The depth distribution of SPOM did not mirror the corresponding nitrate $\delta^{15}\text{N}$ profile, as could otherwise
1197 be expected. At the stratified near-surface (5 m) at station 1, the $\delta^{15}\text{N}$ of SPOM averaged 4.2 ‰ compared to 7.4
1198 ‰ for nitrate. **In the context of Rayleigh fractionation, this result suggests that particulate material at the surface**
1199 **consisted primarily of the instantaneous product of nitrate assimilation (Mariotti et al., 1981). The lower $\delta^{15}\text{N}$**
1200 **SPOM values could also reflect some degree of reliance on regenerated N species, which would result in $\delta^{15}\text{N}$ of**
1201 **SPOM lower than that of incident nitrate (Fawcett et al., 2011; Lourey et al., 2003; Treibergs et al., 2014).**
1202 Deeper in the water column, the $\delta^{15}\text{N}$ of SPOM converged on the $\delta^{15}\text{N}$ of incident nitrate, **between 6 and 7‰,**
1203 **suggesting that SPOM derived from the complete consumption of an incident nitrate pool (even though nitrate**
1204 **was present at these depths). Phytoplankton at these depths may thus have originated from surface water**
1205 **entrained from the Strait of Georgia – where nitrate was completely utilized. The above dynamics complicate**
1206 **validation of the offset between $\delta^{15}\text{N}$ of exported PON and coral-bound $\delta^{15}\text{N}$. Yet we find little evidence for**
1207 **nitrate fractionation from partial assimilation on $\delta^{15}\text{N}$ of phytoplankton SPOM, which suggests that the $\delta^{15}\text{N}$**
1208 **imparted on local *B. elegans* skeletons should reflect the $\delta^{15}\text{N}$ of nitrate entrained to the surface. The ~7‰**
1209 **difference between coral skeleton $\delta^{15}\text{N}$ (~13.5‰) and the entrained nitrate (~6.5‰) is similar to the empirical**
1210 **range of 7 - 9‰ reported for other CWC species. (e.g. *D. petusa*, Kiriakoulakis et al., 2005) and *D. dianthus***
1211 **(Wang et al. 2014), and suggests that *B. elegans* provides a record of the thermocline nitrate $\delta^{15}\text{N}$ and surface**
1212 **nutrient dynamics at Friday Harbor.**

1213 5. Conclusions and implications for paleo-reconstruction from coral $\delta^{15}\text{N}$

1214 We conclude that the solitary scleractinian cold water coral *B. elegans* in Friday Harbor, WA predominantly
1215 derives nutrition from metazoan zooplankton prey. While our study was limited to a shallow field site, our
1216 isotope feeding experiment, evaluated alongside previously published studies, points to the possibility that
1217 deeper-dwelling CWCs could also rely on zooplankton prey as a fundamental component of their diet. SPOM
1218 may contribute to these CWCs' diet, but it cannot be presumed to exclusively account for the large offset
1219 between $\delta^{15}\text{N}$ of PON export and coral skeleton $\delta^{15}\text{N}$ documented by Wang et al. (2014). The $\delta^{15}\text{N}$ of skeletal
1220 material recovered from coral archives is thus likely to be sensitive to local food web dynamics; for a given $\delta^{15}\text{N}$
1221 of sinking PON exiting the surface ocean, the $\delta^{15}\text{N}$ recorded by CWC may differ among individuals of the same

Formatted: Line spacing: 1.5 lines

Deleted: ...result suggesting...that particulate material at the surface consisted primarily of the instantaneous product of nitrate assimilation (Mariotti et al., 1981). The lower $\delta^{15}\text{N}$ SPOM values could also reflect some degree of reliance on regenerated N species, whose ...hich would result in $\delta^{15}\text{N}$ is ...f SPOM generally (... [20])

Formatted: Font color: Text 1

Deleted: The ...he above dynamics complicate validation of the offset between $\delta^{15}\text{N}$ nitrate (... [21])

Formatted

Deleted: . Nevertheless, the offset between nitrate $\delta^{15}\text{N}$ and coral skeleton $\delta^{15}\text{N}$ was on the order of ~6.5 ‰, ...imilar to the empirical range of 7 - 9‰ observed (... [23])

Deleted: *Lophelia* p.;

Deleted: (

Formatted: Font color: Text 1

Formatted

Formatted (... [24])

Deleted: , suggesting that the $\delta^{15}\text{N}$ imparted on local *B. elegans* skeletons reflects the $\delta^{15}\text{N}$ of nitrate entrained to the surface,

Deleted: . The 1.5 - 2 ‰ difference between the 7‰ offset reported here and that by Wang et al. (8-9‰) might stem from either natural variability between CWC species or the effect of coral habitat depth on the magnitude of the offset. Most of the specimens used in Wang et al. calibration study were collected between ~500 and 1500 m depth and these authors found a small, 1-2‰, increase in the offset magnitude with the depth of coral growth, relatively unaltered by surface nitrate fractionation from partial assim (... [25])

Deleted: may be able to

Deleted: ...urface nutrient dynamics ocean processes (... [26])

Deleted: .

Formatted

Formatted (... [27])

Deleted: in Friday Harbor, WA

Deleted: shallower-dwelling organisms

Formatted: Font color: Text 1

Formatted: Font color: Text 1

Deleted: a review of related

Formatted: Font color: Text 1

Deleted: studies corroborates that while

Deleted: may

Deleted: be able to feed on a variety of substrates, other s (... [28])

Deleted: , even at abyssal depths

Formatted: Font color: Text 1

Formatted: Font color: Text 1

Formatted: Font color: Text 1

Deleted: intrinsically ...xclusively account for the large o (... [29])

1318 species feeding on different zooplankton prey, depending on availability. In fact, Wang et al. (2014) did report a
1319 “natural variability” of 1-1.5‰ within a single specimen that might have resulted from some variability of the
1320 local food web on a short time scale of few years. Some studies have documented an increase in the degree of
1321 carnivory of zooplankton with depth (Dodds et al., 2009; Vinogradov, 1962). For instance, Hannides et al. (2013)
1322 recorded a 3.5 ‰ increase in zooplankton $\delta^{15}\text{N}$ from 150 m to 1000 m in the Subtropical North Pacific, with the
1323 steepest rate of increase from 100 – 300 m. Koppelman et al. (2009) reported a similar pattern of
1324 zooplankton $\delta^{15}\text{N}$ through the water column. These findings could explain previous reports of small but
1325 resolvable (1-2 ‰) depth-dependencies of coral $\delta^{15}\text{N}$ (Wang et al. 2014) if corals feed predominantly on
1326 zooplankton with depth-dependent degree of carnivory of zooplankton and increasing with depth $\delta^{15}\text{N}$. The $\delta^{15}\text{N}$
1327 recorded in CWC skeletons also tends to differ among species by 1-2‰, as respective species occupy different
1328 nutritional niches (Teece et al., 2011). The relationship between CWC species represented in fossil archives to
1329 the depth structure of their zooplankton prey warrants further investigation.

1330 Consideration of the possible dependence of coral-bound $\delta^{15}\text{N}$ on food web dynamics informs the questions
1331 that can be competently addressed by this proxy. Although we do not have direct estimates of the $\delta^{15}\text{N}$ range that
1332 can be expected from local food web variability, the scatter around the global compilation of Wang et al. (2014)
1333 for coral-bound $\delta^{15}\text{N}$ of *D. dianthus* relative to the $\delta^{15}\text{N}$ of PON suggests that this range is modest, on the order of
1334 ~1-2 ‰. Given this range, we suggest that the coral-bound $\delta^{15}\text{N}$ proxy will be most useful for reconstructing
1335 larger environmental $\delta^{15}\text{N}$ signals and where chosen coral samples belong to the same species and are collected at
1336 comparable depths as has already been successfully demonstrated by Wang et al. (2017), Studer et al. (2018) and
1337 Chen et al. (2023). If used in this way, the broad geographic and temporal coverage afforded by CWCs, the
1338 opportunity to measure multiple proxies from individual specimens and the imperviousness of coral-bound $\delta^{15}\text{N}$
1339 to diagenetic alteration render it a valuable paleo-proxy for reconstructing marine N cycling.

1341 **Data Availability** Data presented in this paper is available at: <https://www.bco-dmo.org/project/893811>.

1343 **Author Contribution** JG, AG, and MP conceptualized the research presented in this paper. JM and AG designed
1344 and carried out culture experiments. MP and AC prepared coral samples for analysis. JM and VR analyzed
1345 samples. JM, AG, JG and KD collected water samples, SPOM, and net tows. KD collected live corals for culture
1346 experiments and field studies. JM and JG prepared the manuscript with contributions from all co-authors.

1348 **Competing Interests:** The authors declare that they have no conflict of interest.

Deleted: food ...availability. In fact, Wang et al. (2014) did report a “natural variability” of 1-1.5‰ within a single specimen that might have resulted from some variability of the local food web on a short time scale of few years. Additionally, s (... [30])

Deleted: In this regard, the depth at which corals reside may be an important determinant of their trophic level, due to a...documented an increase in the degree of carnivory of zooplankton with depth (Dodds et al., 2009; Vinogradov, 1962)... For instance, Hannides et al. (2013) recorded a 3.5 ‰ increase in zooplankton $\delta^{15}\text{N}$ from 150 m to 1000 m in the Subtropical North Pacific, with the steepest rate of increase from 100 – 300 m. Koppelman et al. (2009) reported a similar pattern of zooplankton $\delta^{15}\text{N}$ (... [31])

Deleted: studies

Deleted: suggest...ould explain that (... [32])

Formatted: Font color: Text 1

Formatted: Font color: Text 1

Deleted: y

Deleted: could also vary with depth...if they are feeding...predominantly on zooplankton with depth-dependent degree of carnivory of zooplankton and increasing with depth $\delta^{15}\text{N}$. (Wang et al. 2014). ...he $\delta^{15}\text{N}$ recorded in CWC skeletons is (... [33])

Formatted: Font color: Text 1

Formatted: Font color: Text 1

Deleted: We note that t

Deleted: sensitivity ...ossible dependence of the (... [34])

Deleted: to

Deleted: adroitly ...ompetently addressed with ...y these...proxy... and the relationship of CWC species represented in fossil archives to the depth structure of zooplankton prey warrants further investigation. ...Although we do not have direct estimates of the $\delta^{15}\text{N}$ range that can be expected from local food web variability, the scatter around the global compilation of Wang et al. (2014) for coral-bound $\delta^{15}\text{N}$ of *D. dianthus* relative to the $\delta^{15}\text{N}$ of PON suggests that this range is modest, on the order of ~1-2 ‰. Given this range, we suggest that the coral-bound $\delta^{15}\text{N}$ proxy is most useful in systems...ill be most useful for reconstructing larger (... [35])

Deleted: come from

Deleted: correspond

Formatted

Deleted: (e.g., (... [36])

Deleted: ;

Formatted

Formatted: Font color: Text 1 (... [37])

Formatted: Font color: Text 1

Formatted: Font color: Text 1

Formatted: Indent: First line: 0", Line spacing: 1.5 lines

Deleted: ¶ (... [38])

Formatted: Font color: Text 1

Formatted: Font color: Text 1

1462 **Acknowledgements**

1463 We are grateful to Friday Harbor Labs for their assistance with coral collections and field sampling, especially
1464 Pema Kitaeff and Megan Dethier. We acknowledge the valued assistance of the Artemia Reference Center
1465 (specifically Gilbert Van Stappen and Christ Mahieu). Coral culture experiments would not have been sustained
1466 without the help of St. Olaf undergraduate students Rachel Raser, Joash Daniel, Qintiantian Nong, YiWynn
1467 Chan, Mansha Haque, [Natasia Preys](#) and Miranda Lenz. We are also indebted to Dr. C. Tobias and P. Ruffino for
1468 access to and assistance with the Elemental Analyzer Isotope Ratio Mass Spectrometer. This project was
1469 funded by an NSF RUI award to A.G. (OCE-1949984), M.G.P. (OCE-1949132) and J.G. (OCE-1949119).

1471 **References**

1472 Adams, T.S., Sterner, R.W. 2000. The effect of dietary nitrogen content on trophic level ¹⁵N enrichment. *Limnol.*
1473 *Oceanogr.* 45, 601–607. <https://doi.org/10.4319/lo.2000.45.3.0601>

1474 Adkins, J.F., Henderson, G.M., Wang, S.-L., O’Shea, S., Mokadem, F. 2004. Growth rates of the deep-sea
1475 Scleractinia *Desmophyllum cristagalli* and *Enallopsammia rostrata*. *Earth and Planetary Science Letters*
1476 227, 481–490. <https://doi.org/10.1016/j.epsl.2004.08.022>

1477 Al-Moghrabi, S., Allemand, D. & Jaubert, J. 1993. Valine uptake by the scleractinian coral *Galaxea fascicularis*:
1478 characterization and effect of light and nutritional status. *J Comp Physiol B* 163, 355–362.
1479 <https://doi.org/10.1007/BF00265638>

1480 Altabet, M.A., 1988. Variations in nitrogen isotopic composition between sinking and suspended particles:
1481 implications for nitrogen cycling and particle transformation in the open ocean. *Deep Sea Res. Part*
1482 *Oceanogr. Res. Pap.* 35, 535–554. [https://doi.org/10.1016/0198-0149\(88\)90130-6](https://doi.org/10.1016/0198-0149(88)90130-6)

1483 Altabet, M.A., Deuser, W.G., Honjo, S., Stienen, C., 1991. Seasonal and depth-related changes in the source of
1484 sinking particles in the North Atlantic. *Nature* 354, 136–139. <https://doi.org/10.1038/354136a0>

1485 Altabet, M.A., Francois, R., 1994. Sedimentary nitrogen isotopic ratio as a recorder for surface ocean nitrate
1486 utilization. *Glob. Biogeochem. Cycles* 8, 103–116. <https://doi.org/10.1029/93GB03396>

1487 Altabet, M., Higgingson, M. & Murray, D. 2002. The effect of millennial-scale changes in Arabian Sea
1488 denitrification on atmospheric CO₂. *Nature* 415, 159–162. <https://doi.org/10.1038/415159a>

1489 Ayliffe, L.K., Cerling, T.E., Robinson, T., West, A.G., Sponheimer, M., Passey, B.H., Hammer, J., Roeder, B.,
1490 Dearing, M.D., Ehleringer, J.R., 2004. Turnover of carbon isotopes in tail hair and breath CO₂ of horses
1491 fed an isotopically varied diet. *Oecologia* 139, 11–22. <https://doi.org/10.1007/s00442-003-1479-x>

1492 Banas, N., Bricker, J., Carter, G., Gerdes, F., Martin, W., Nelson, E., Ross, T., Scansen, B., Simons, R., Wells,
1493 M., 1999. Flow, Stratification, and mixing in San Juan Channel.

1494 [Beauchamp, K.A., 1989. Aspects of gametogenesis, development and planulation in laboratory populations of
1495 solitary corals and corallimorpharian sea anemones \(Ph.D.\). University of California, Santa Cruz, United
1496 States -- California.](#)

1497 Böhlke, J.K., Mroczkowski, S.J., Coplen, T.B., 2003. Oxygen isotopes in nitrate: new reference materials for
1498 18O:17O:16O measurements and observations on nitrate-water equilibration. *Rapid Commun. Mass*
1499 *Spectrom.* RCM 17, 1835–1846. <https://doi.org/10.1002/rcm.1123>

Deleted: u

Formatted: Font color: Text 1

Formatted: Font color: Text 1

Formatted: Font color: Text 1

Formatted: Font color: Text 1

Formatted: Font color: Text 1

Deleted: Alldredge, A.L., King, J.M., 1977. Distribution, abundance, and substrate preferences of demersal reef zooplankton at Lizard Island Lagoon, Great Barrier Reef. *Mar. Biol.* 41, 317–333. <https://doi.org/10.1007/BF00389098>

Formatted: Font color: Text 1

Formatted: Font color: Text 1

Formatted: Font color: Text 1

Formatted: Font color: Text 1

Formatted: Font color: Text 1

Formatted: Font color: Text 1

Formatted: Font: 11 pt, Font color: Text 1

Formatted: Normal, Indent: Left: 0", Hanging: 0.5", Space Before: 0 pt, After: 0 pt

Formatted: Font color: Text 1

Formatted: Font color: Text 1

Formatted: Font color: Text 1

1505 Braman, R.S., Hendrix, S.A., 1989. Nanogram nitrite and nitrate determination in environmental and biological
 1506 materials by vanadium(III) reduction with chemiluminescence detection. *Anal. Chem.* 61, 2715–2718.
 1507 <https://doi.org/10.1021/ac00199a007>

1508 Brandes, J.A., Devol, A.H., 2002. A global marine-fixed nitrogen isotopic budget: Implications for Holocene
 1509 nitrogen cycling. *Glob. Biogeochem. Cycles* 16, 67-1-67–14. <https://doi.org/10.1029/2001GB001856>

1510 Bronk, D. A. 2002. Dynamics of DON. *Biogeochem. Mar. Dissolved Org. Matter* 153–249.

1511 Brown, B. E., & Bythell, J. C. 2005. Perspectives on mucus secretion in reef corals. *Marine Ecology Progress
 1512 Series*, 296, 291–309. <http://www.jstor.org/stable/24868640> Cairns, S.D., 2007. Deep-water corals: an
 1513 overview with special reference to diversity and distribution of deep-water scleractinian corals. *Bull.
 1514 Mar. Sci.* 81, 311–322.

1515 Carlier, A., Guilloux, E.L., Olu, K., Sarrazin, J., Mastrototaro, F., Taviani, M., Clavier, J., 2009. Trophic
 1516 relationships in a deep Mediterranean cold-water coral bank (Santa Maria di Leuca, Ionian Sea). *Mar.
 1517 Ecol. Prog. Ser.* 397, 125–137. <https://doi.org/10.3354/meps08361>

1518 Carpenter, E. J., Harvey, H. R., Fry, B. & Capone, D. G. 1997. Biogeochemical tracers of the marine
 1519 cyanobacterium *Trichodesmium*. *Deep-Sea Res. I* 44, 27–38. [doi.org/10.1016/S0967-0637\(96\)00091-X](https://doi.org/10.1016/S0967-0637(96)00091-X)

1520 Casciotti, K.L., Sigman, D.M., Hastings, M.G., Böhlke, J.K., Hilkert, A., 2002. Measurement of the oxygen
 1521 isotopic composition of nitrate in seawater and freshwater using the denitrifier method. *Anal. Chem.* 74,
 1522 4905–4912. <https://doi.org/10.1021/ac020113w>

1523 Casciotti, K.L., Trull, T.W., Glover, D.M., Davies, D., 2008. Constraints on nitrogen cycling at the subtropical
 1524 North Pacific Station ALOHA from isotopic measurements of nitrate and particulate nitrogen. *Deep Sea
 1525 Res. Part II Top. Stud. Oceanogr.* 55, 1661–1672. <https://doi.org/10.1016/j.dsr2.2008.04.017>

1526 Cathalot C, Van Oevelen D, Cox TJS, Kutti T., Lavaleye M., Duineveld G., Meysman F. J. R. 2015. Cold-water
 1527 coral reefs and adjacent sponge grounds: hotspots of benthic respiration and organic carbon cycling in the
 1528 deep sea. *Front Mar Sci* 2. <https://www.frontiersin.org/articles/10.3389/fmars.2015.00037>.

1529 Cerling, T.E., Ayliffe, L.K., Dearing, M.D., Ehleringer, J.R., Passey, B.H., Podlesak, D.W., Torregrossa, A-M.,
 1530 West, A.G. 2007. Determining biological tissue turnover using stable isotopes: the reaction progress
 1531 variable. *Ecophysiology* 151, 175-189. <https://doi.org/10.1007/s00442-006-0571-4>

1532 Chen, WH., Ren, H., Chiang, J.C.H. *et al.* Increased tropical South Pacific western boundary current transport
 1533 over the past century. *Nat. Geosci.* 16, 590–596 (2023). <https://doi.org/10.1038/s41561-023-01212-4>

1534 Cheng, H., Adkins, J., Edwards, R.L., Boyle, E.A., 2000. U-Th dating of deep-sea corals. *Geochim. Cosmochim.
 1535 Acta* 64, 2401–2416. [https://doi.org/10.1016/S0016-7037\(99\)00422-6](https://doi.org/10.1016/S0016-7037(99)00422-6)

1536 Crook, E.D., Cooper, H., Potts, D.C., Lambert, T., Paytan, A., 2013. Impacts of food availability and pCO₂ on
 1537 planulation, juvenile survival, and calcification of the azooxanthellate scleractinian coral *Balanophyllia
 1538 elegans*. *Biogeosciences* 10, 7599–7608. <https://doi.org/10.5194/bg-10-7599-2013>

1539 Da Ros, Z., Dell’Anno, A., Fanelli, E., Angeletti, L., Taviani, M., Danovaro, R., 2022. Food preferences of
 1540 Mediterranean cold-water corals in captivity. *Front. Mar. Sci.* 9.

1541 Del Bel Belluz, J., Peña, M.A., Jackson, J.M., Nemcek, N., 2021. Phytoplankton composition and environmental
 1542 drivers in the Northern Strait of Georgia (Salish Sea), British Columbia, Canada. *Estuaries Coasts* 44,
 1543 1419–1439. <https://doi.org/10.1007/s12237-020-00858-2>

Formatted: No underline, Font color: Text 1

Formatted: Font: 11 pt, Font color: Text 1

Formatted: Font color: Text 1

Formatted: Font: 11 pt, Font color: Text 1

Formatted: Font color: Text 1

Formatted: Normal, Space Before: 0 pt, After: 0 pt

Formatted: Font color: Text 1

Formatted: Font color: Text 1

Formatted: Font color: Text 1

Formatted: Font color: Text 1

Formatted: Font color: Text 1

Formatted: Font color: Text 1

Formatted: Font color: Text 1

Formatted: Font color: Text 1

Deleted: Cohen, A.L., Gaetani, G.A., Lundålv, T., Corliss, B.H., George, R.Y., 2006. Compositional variability in a cold-water scleractinian, *Lophelia pertusa*: New insights into vital effects. *Geochem. Geophys. Geosystems* 7. <https://doi.org/10.1029/2006GC001354>
 Corbera, G., Lo Iacono, C., Simarro, G. *et al.* 2022. Local-scale feedbacks influencing cold-water coral growth and subsequent reef formation. *Sci. Rep.* 12, 20389. <https://doi.org/10.1038/s41598-022-24711-7>

Formatted: Font color: Text 1

Formatted: Font color: Text 1

Formatted: Font color: Text 1

- 1553 De Pol-Holz R, Robinson RS, Hebbeln D, Sigman DM, Ulloa O. 2009. Controls on sedimentary nitrogen
 1554 isotopes along the Chile margin. *Deep Res Part II Top Stud Oceanogr* 56(16).
 1555 doi:10.1016/j.dsr2.2008.09.014
- 1556 DiFiore, P.J., Sigman, D.M., Trull, T.W., Lourey, M.J., Karsh, K., Cane, G., Ho, R., 2006. Nitrogen isotope
 1557 constraints on subantarctic biogeochemistry. *J. Geophys. Res. Oceans* 111.
 1558 <https://doi.org/10.1029/2005JC003216>
- 1559 Dodds, L.A., Black, K.D., Orr, H., Roberts, J.M., 2009. Lipid biomarkers reveal geographical differences in food
 1560 supply to the cold-water coral *Lophelia pertusa* (Scleractinia). *Mar. Ecol. Prog. Ser.* 397, 113–124.
 1561 <https://doi.org/10.3354/meps08143>
- 1562 Doi, H., Akamatsu, F., González, A.L., 2017. Starvation effects on nitrogen and carbon stable isotopes of
 1563 animals: an insight from meta-analysis of fasting experiments. *R. Soc. Open Sci.* 4, 170633.
 1564 <https://doi.org/10.1098/rsos.170633>
- 1565 Drake, J.L., Guillermic, M., Eagle, R.A., Jacobs, D.K., 2021. Fossil corals with various degrees of preservation
 1566 can retain information about biomineralization-related organic material. *Front. Earth Sci.* 9.
- 1567 Druffel, E.R.M., 1997. Geochemistry of corals: Proxies of past ocean chemistry, ocean circulation, and climate.
 1568 *Proc. Natl. Acad. Sci.* 94, 8354–8361. <https://doi.org/10.1073/pnas.94.16.8354>
- 1569 Duineveld, G.C.A., Lavaleye, M.S.S., Berghuis, E.M., 2004. Particle flux and food supply to a seamount cold-
 1570 water coral community (Galicia Bank, NW Spain). *Mar. Ecol. Prog. Ser.* 277, 13–23.
 1571 <https://doi.org/10.3354/meps277013>
- 1572 Duineveld, G., Lavaleye, M., Bergman, M., Stigter, H., Mienis, F., 2007. Trophic structure of a cold-water coral
 1573 mound community (Rockall Bank, NE Atlantic) in relation to the near-bottom particle supply and current
 1574 regime. *Bull. Mar. Sci.* 81, 449–467.
- 1575 **Durham, J. W., and Barnard, J.L., 1952. Stony corals of the Eastern Pacific collected by the Velero III
 1576 and Velero IV. All an Hancock Pacific Expeditions 16, 1-110.**
- 1577 Erler, D.V., Wang, X.T., Sigman, D.M., Scheffers, S.R., Shepherd, B.O., 2015. Controls on the nitrogen isotopic
 1578 composition of shallow water corals across a tropical reef flat transect. *Coral Reefs* 34, 329–338.
 1579 <https://doi.org/10.1007/s00338-014-1215-5>
- 1580 Esri. "Ocean" [basemap]. Scale Not Given. " Ocean Basemap ". February 11, 2021.
 1581 [https://hub.arcgis.com/maps/CESPK::ocean-basemap/explore?location=35.956244%2C-
 1582 111.078800%2C5.00](https://hub.arcgis.com/maps/CESPK::ocean-basemap/explore?location=35.956244%2C-111.078800%2C5.00). (December, 2022).
- 1583 Fadlallah, Y.H., 1983. Population Dynamics and Life History of a Solitary Coral, *Balanophyllia elegans*, from
 1584 Central California. *Oecologia* 58, 200–207.
- 1585 Fautin, D.G., 2009. Structural diversity, systematics, and evolution of cnidae. *Toxicon, Cnidarian Toxins and
 1586 Venoms* 54, 1054–1064. <https://doi.org/10.1016/j.toxicon.2009.02.024>
- 1587 Fawcett, S.E., Lomas, M.W., Casey, J.R., Ward, B.B., Sigman, D.M., 2011. Assimilation of upwelled nitrate by
 1588 small eukaryotes in the Sargasso Sea. *Nat. Geosci.* 4, 717–722. <https://doi.org/10.1038/ngeo1265>
- 1589 Ferrier, M.D. 1991. Net uptake of dissolved free amino acids by four scleractinian corals. *Coral Reefs* 10, 183–
 1590 187. <https://doi.org/10.1007/BF00336772>

Formatted: Font color: Text 1

Formatted: Font color: Text 1

Formatted: Font color: Text 1

Formatted: Font color: Text 1

Deleted: Duineveld GCA, Jeffreys RM, Lavaleye MSS, Davies AJ, Bergman MIN, Watmough T, Witbaard R. 2012. Spatial and tidal variation in food supply to shallow cold-water coral reefs of the Mingulay Reef complex (Outer Hebrides, Scotland). *Mar Ecol Prog Ser* 444:97–115. <https://doi.org/10.3354/meps09430>

Formatted: Font color: Text 1

Formatted: Font color: Text 1

Formatted: Font color: Text 1

Formatted: Font color: Text 1

Formatted: Font color: Text 1

Formatted: Font color: Text 1

- 1596 François, R., Altabet, M.A., Yu, E.-F., Sigman, D.M., Bacon, M.P., Frank, M., Bohrmann, G., Bareille, G.,
 1597 Labeyrie, L.D., 1997. Contribution of Southern Ocean surface-water stratification to low atmospheric
 1598 CO2 concentrations during the last glacial period. *Nature* 389, 929–935. <https://doi.org/10.1038/40073>
- 1599 Freiwald, A. 2002. Reef-Forming Cold-Water Corals. In: Wefer, G., Billett, D., Hebbeln, D., Jørgensen, B.B.,
 1600 Schlüter, M., van Weering, T.C.E. (eds) *Ocean Margin Systems*. Springer, Berlin, Heidelberg.
 1601 https://doi.org/10.1007/978-3-662-05127-6_23
- 1602 Gagnon, A.C., Gothmann, A.M., Branson, O., Rae, J.W.B., Stewart, J.A., 2021. Controls on boron
 1603 isotopes in a cold-water coral and the cost of resilience to ocean acidification. *Earth and*
 1604 *Planetary Science Letters* 554, 116662. <https://doi.org/10.1016/j.epsl.2020.116662>
- 1605 Ganeshram, R. S., and Pedersen, T. F. 1998, Glacial-interglacial variability in upwelling and bioproductivity off
 1606 NW Mexico: Implications for Quaternary paleoclimate, *Paleoceanography*, 13(6), 634– 645,
 1607 doi:10.1029/98PA02508.
- 1608 Garcia-Herrera, N., Cornils, A., Laudien, J., Niehoff, B., Höfer, J., Försterra, G., González, H.E.,
 1609 Richter, C., 2022. Seasonal and diel variations in the vertical distribution, composition,
 1610 abundance and biomass of zooplankton in a deep Chilean Patagonian Fjord. *PeerJ* 10, e12823.
 1611 <https://doi.org/10.7717/peerj.12823>
- 1612 Genin, A., Dayton, P.K., Lonsdale, P.F., Spiess, F.N., 1986. Corals on seamount peaks provide
 1613 evidence of current acceleration over deep-sea topography. *Nature* 322, 59–61.
 1614 <https://doi.org/10.1038/322059a0>
- 1615 Gerrodette, T. 1981. Equatorial Submergence in a Solitary Coral, *Balanophyllia elegans*, and the
 1616 Critical Life Stage Excluding the Species from Shallow Water in the South. *Mar. Ecol. Prog.*
 1617 *Series 1*, 227-235. <http://www.jstor.org/stable/24812947>.
- 1618 Gonfiantini, R., W. Stichler, and K. Rosanski 1995, Standards and Intercomparison. Materials
 1619 Distributed by the IAEA for Stable Isotope Measurements, Int. At. Energy Agency, Vienna.
- 1620 Goodfriend, G.A., Hare, P.E., Druffel, E.R.M. 1992. Aspartic acid racemization and protein diagenesis
 1621 in corals over the last 350 years. *Geochim. Cosmochim. Acta* 56, 3847–3850.
 1622 [https://doi.org/10.1016/0016-7037\(92\)90176-J](https://doi.org/10.1016/0016-7037(92)90176-J)
- 1623 Gori, A., R. Grover, C. Orejas, S. Sikorski, and C. Ferrier-Pagès. 2014. Uptake of dissolved free amino
 1624 acids by four cold-water coral species from the Mediterranean Sea. *Deep Sea Res. Part II Top.*
 1625 *Stud. Oceanogr.* 99: 42–50. doi:10.1016/j.dsr2.2013.06.007.
- 1627 Gothmann AM, Stolarski J, Adkins JF, et al. Fossil corals as an archive of secular variations in seawater
 1628 chemistry since the Mesozoic. *Geochim Cosmochim Acta*. 2015;160:188-208.
 1629 doi:https://doi.org/10.1016/j.gca.2015.03.018
- 1630 Grover, R. Maguer, J-F, Allemand, D., Ferrier-Pagès, C. 2008. Uptake of dissolved free amino acids by the
 1631 scleractinian coral *Stylophora pistillata*. *J Exp Biol* 211 (6): 860–865. doi:
 1632 <https://doi.org/10.1242/jeb.012807>

Formatted: Font color: Text 1

Formatted: Font color: Text 1

Formatted: Font color: Text 1

Formatted: Normal, Indent: Left: 0", Hanging: 0.5", Space Before: 0 pt, After: 0 pt

Deleted: ¶

Formatted: Font: 12 pt, Font color: Text 1

Formatted: Font color: Text 1

Formatted: Font: 12 pt, Font color: Text 1

Formatted: Font color: Text 1

Formatted: Font: 12 pt, Font color: Text 1

Formatted: Font: (Default) Times New Roman, 12 pt, Font color: Text 1

Formatted: Font: (Default) Times New Roman, 12 pt, No underline, Font color: Text 1

Formatted: Font: (Default) Times New Roman, 12 pt, Font color: Text 1

Formatted: Font: (Default) Times New Roman, Font color: Text 1

Formatted: Bibliography, Space Before: 0.6 line, After: 0.6 line

Formatted: Underline, Font color: Text 1

Deleted: ¶

Formatted: Font: (Default) Times New Roman, 12 pt, Font color: Text 1

Formatted: Font: (Default) Times New Roman, 12 pt, No underline, Font color: Text 1

Formatted: Font: 12 pt, Font color: Text 1

Formatted: Font color: Text 1

Formatted: Font: +Body (Times New Roman), Font color: Text 1

Formatted: Font color: Text 1

Formatted: ... [39]

Formatted: Space Before: 0 pt, After: 0 pt

Deleted: ¶

Formatted: ... [40]

Formatted: Font: 12 pt, Font color: Text 1

Formatted: Font color: Text 1

Deleted: Renaud

Formatted: Font color: Text 1

Formatted: Font color: Text 1

Formatted: Font color: Text 1

- 1637 Hannides, Cecelia C. S., Popp, Brian N., Choy, C. Anela, Drazen, Jeffrey C. 2013. Midwater zooplankton and
 1638 suspended particle dynamics in the North Pacific Subtropical Gyre: A stable isotope perspective,
 1639 *Limnology and Oceanography*, 58, doi: 10.4319/lo.2013.58.6.1931.
- 1640 Hill, T.M., Myrvold, C.R., Spero, H.J., Guilderson, T.P. 2014. Evidence for benthic and pelagic food web
 1641 coupling and carbon export from California margin bamboo coral archives. *Biogeosciences* 11, 3845–
 1642 3854. <https://doi.org/10.5194/bg-11-3845-2014>.
- 1643 Hines, S.K.V., Southon, J.R., Adkins, J.F. 2015. A high-resolution record of Southern Ocean intermediate water
 1644 radiocarbon over the past 30,000 years. *Earth and Planetary Science Letters* 432, 46–58.
 1645 <https://doi.org/10.1016/j.epsl.2015.09.038>.
- 1646 Hoegh-Guldberg, O., Williamson, J. Availability of two forms of dissolved nitrogen to the coral *Pocillopora*
 1647 *damicornis* and its symbiotic zooxanthellae. *Marine Biology* 133, 561–570 (1999).
 1648 <https://doi.org/10.1007/s002270050496>
- 1649 Höfer, J., González, H.E., Laudien, J., Schmidt, G.M., Häussermann, V., Richter, C., 2018. All you can eat: the
 1650 functional response of the cold-water coral *Desmophyllum dianthus* feeding on krill and copepods. *PeerJ*
 1651 6, e5872. <https://doi.org/10.7717/peerj.5872>
- 1652 Horn, M.G., Robinson, R.S., Rynearson, T.A., Sigman, D.M., 2011. Nitrogen isotopic relationship between
 1653 diatom-bound and bulk organic matter of cultured polar diatoms. *Paleoceanography* 26.
 1654 <https://doi.org/10.1029/2010PA002080>.
- 1655 Kast, E.R., Stolper, D.A., Auderset, A., Higgins, J.A., Ren, H., Wang, X.T., Martínez-García, A., Haug, G.H.,
 1656 Sigman, D.M., 2019. Nitrogen isotope evidence for expanded ocean suboxia in the early Cenozoic.
 1657 *Science* 364, 386–389. <https://doi.org/10.1126/science.aau5784>
- 1658 Kiriakoulakis, K., Fisher, E., Wolff, G.A., Freiwald, A., Grehan, A., Roberts, J.M., 2005. Lipids and nitrogen
 1659 isotopes of two deep-water corals from the North-East Atlantic: initial results and implications for their
 1660 nutrition, in: Freiwald, A., Roberts, J.M. (Eds.), *Cold-Water Corals and Ecosystems*, Erlangen Earth
 1661 Conference Series. Springer, Berlin, Heidelberg, pp. 715–729. https://doi.org/10.1007/3-540-27673-4_37.
- 1662 Knapp, A. N., K. L. Casciotti, and M. G. Prokopenko. 2018. Dissolved Organic Nitrogen Production
 1663 and Consumption in Eastern Tropical South Pacific Surface Waters. *Glob. Biogeochem. Cycles*
 1664 32: 769–783. doi:10.1029/2017GB005875.
- 1665 Knapp AN, DiFiore PJ, Deutsch C, Sigman DM, Lipschultz F. 2008. Nitrate isotopic composition between
 1666 Bermuda and Puerto Rico: Implications for N₂ fixation in the Atlantic Ocean. *Global Biogeochem Cycles*
 1667 22(3). doi:10.1029/2007GB003107
- 1668 Koppelman, R., Böttger-Schnack, R., Möbius, J., Weikert, H., 2009. Trophic relationships of zooplankton in the
 1669 eastern Mediterranean based on stable isotope measurements. *Journal of Plankton Research* 31, 669-686.
- 1670 Lasker, H.R., 1981. A comparison of the particulate feeding abilities of three species of Gorgonian soft coral.
 1671 *Mar. Ecol. Prog. Ser.* 5, 61–67.
- 1672 Lewis, A.G., 1978. Concentrations of nutrients and chlorophyll on a cross-channel transect in Juan de Fuca Strait,
 1673 British Columbia. *J. Fish. Res. Board Can.* 35, 305–314. <https://doi.org/10.1139/f78-055>

Formatted: Font color: Text 1

Formatted: No underline, Font color: Text 1

Formatted: Font color: Text 1

Formatted: Font color: Text 1

Formatted: Font color: Text 1

Formatted: Font color: Text 1

Formatted: Font color: Text 1

Formatted: Font color: Text 1

Formatted: Font color: Text 1

Formatted: Font color: Text 1

Formatted: Font color: Text 1

Deleted: Houlière F, Tambutti E, Allemand D, Ferrier-Pagès C. 2004. Interactions between zooplankton feeding, photosynthesis and skeletal growth in the scleractinian coral *Stylophora pistillata*. *J Exp Biol.* 4 Apr;207(Pt 9):1461-9. doi: 10.1242/jeb.009111. PMID: 15037640.

Formatted: Font color: Text 1

Formatted: No underline, Font color: Text 1

Formatted: Font color: Text 1

Formatted: Font color: Text 1

Formatted: Bibliography, Space Before: 0.6 line, After: 0.6 line

Formatted: Font: 11 pt, Underline, Font color: Text 1

Deleted: ¶

Formatted: Font color: Text 1

Deleted: <inf>2</inf>

Formatted: Font color: Text 1

Deleted: ¶

Deleted: Kuanui P, Chavanich S, Viyakam V, Omori M, Fujita T, Lin C. 2020. Effect of light intensity on survival and photosynthetic efficiency of cultured corals of different ages. *Estuar Coast Shelf Sci.* 235:106515. doi:<https://doi.org/10.1016/j.eess.2019.106515>
 Knutson, D.W., Buddemeier, R.W., Smith, S.V., 1972. Coral chronometers: Seasonal growth bands in reef corals. *Science* 177, 270–272. <https://doi.org/10.1126/science.177.4045.270>
 Larsson AI, Lundälv T, van Oevelen D. 2013. Skeletal growth, respiration rate and fatty acid composition in the cold-water coral *Lophelia pertusa* under varying food conditions. *Mar Ecol Prog Ser* 483:169–184. <https://doi.org/10.3354/meps10284>

Formatted: Font color: Text 1

1694 Lewis, J.B., Price, W.S., 1975. Feeding mechanisms and feeding strategies of Atlantic reef corals. *J. Zool.* 176,
1695 527–544. <https://doi.org/10.1111/j.1469-7998.1975.tb03219.x>

1696 [Li, T., Robinson, L.F., Chen, T., Wang, X.T., Burke, A., Rae, J.W.B., Pegrum-Haram, A., Knowles,
1697 T.D.J., Li, G., Chen, J., Ng, H.C., Prokopenko, M., Rowland, G.H., Samperiz, A., Stewart, J.A.,
1698 Southon, J., Spooner, P.T., 2020. Rapid shifts in circulation and biogeochemistry of the
1699 Southern Ocean during deglacial carbon cycle events. *Science Advances* 6, eabb3807](#)

1700

1701 Lourey, M.J., Trull, T.W., Sigman, D.M., 2003. Sensitivity of $\delta^{15}\text{N}$ of nitrate, surface suspended and deep
1702 sinking particulate nitrogen to seasonal nitrate depletion in the Southern Ocean. *Glob. Biogeochem.*
1703 *Cycles* 17. <https://doi.org/10.1029/2002GB001973>

1704 Mackas, D.L., Harrison, P.J., 1997. Nitrogenous nutrient sources and sinks in the Juan de Fuca Strait/Strait of
1705 Georgia/Puget Sound estuarine system: Assessing the potential for eutrophication. *Estuar. Coast. Shelf*
1706 *Sci.* 44, 1–21. <https://doi.org/10.1006/ecss.1996.0110>

1707 Maier, S.R., Bannister, R.J., van Oevelen, D., Kutti, T., 2020. Seasonal controls on the diet, metabolic activity,
1708 tissue reserves and growth of the cold-water coral *Lophelia pertusa*. *Coral Reefs* 39, 173–187.
1709 <https://doi.org/10.1007/s00338-019-01886-6>

1710 [Maier, S.R., Kutti, T., Bannister, R.J., van Breugel, P., van Rijswijk, P., van Oevelen, D., 2019. Survival under
1711 conditions of variable food availability: Resource utilization and storage in the cold-water coral *Lophelia*
1712 *pertusa*. *Limnol. Oceanogr.* 64, 1651–1671. <https://doi.org/10.1002/lno.11142>](#)

1713 [Maier, S.R., Brooke, S., De Clippele, L.H., de Froe, E., van der Kaaden, A.-S., Kutti, T., Mienis, F., van Oevelen,
1714 D., 2023. On the paradox of thriving cold-water coral reefs in the food-limited deep sea. *Biological*
1715 *Reviews* 98, 1768–1795. <https://doi.org/10.1111/brv.12976>](#)

1716 [Marconi D., Weigand AM, Rafter PA, Matthew R. McIlvin MR, Matthew Forbes, M Casciotti, KL Sigman, DM.
1717 2015. Nitrate isotope distributions on the US GEOTRACES North Atlantic cross-basin section: Signals of
1718 polar nitrate sources and low latitude nitrogen cycling. *Mar Chem.* 177:143-156.
1719 doi:<https://doi.org/10.1016/j.marchem.2015.06.007>](#)

1720 [Margolin, A. R., L. F. Robinson, A. Burke, R. G. Waller, K. M. Scanlon, M. L. Roberts, M. E. Auro, and T. van
1721 de Fliedtd. 2014. Temporal and spatial distributions of cold-water corals in the Drake Passage: Insights
1722 from the last 35,000 years. *Deep Sea Res. Part II Top. Stud. Oceanogr.* 99: 237–248.
1723 doi:\[10.1016/j.dsr2.2013.06.008\]\(https://doi.org/10.1016/j.dsr2.2013.06.008\)](#)

1724 Mariotti, A., Germon, J.C., Hubert, P., Kaiser, P., Letolle, R., Tardieux, A., Tardieux, P., 1981. Experimental
1725 determination of nitrogen kinetic isotope fractionation: Some principles; illustration for the
1726 denitrification and nitrification processes. *Plant Soil* 62, 413–430. <https://doi.org/10.1007/BF02374138>

1727 Martínez del Río, C., Carleton, S.A., 2012. How fast and how faithful: the dynamics of isotopic incorporation
1728 into animal tissues. *J. Mammal.* 93, 353–359. <https://doi.org/10.1644/11-MAMM-S-165.1>

1729 McCutchan Jr, J.H., Lewis Jr, W.M., Kendall, C., McGrath, C.C., 2003. Variation in trophic shift for stable
1730 isotope ratios of carbon, nitrogen, and sulfur. *Oikos* 102, 378–390. [https://doi.org/10.1034/j.1600-
0706.2003.12098.x](https://doi.org/10.1034/j.1600-

1731 0706.2003.12098.x)

Formatted: Hyperlink, Font: 12 pt, Font color: Auto

Field Code Changed

Formatted: Indent: Left: 0", Hanging: 0.5"

Formatted: Font: 12 pt, Font color: Auto

Formatted: Normal, Space Before: 0 pt, After: 0 pt

Formatted: Font color: Text 1

Formatted: Font color: Text 1

Formatted: Font color: Text 1

~~Deleted: Maier C, Hegeman J, Weinbauer MG, Gattuso J-P. Calcification of the cold-water coral *Lophelia pertusa* under ambient and reduced pH. *Biogeochemistry*. 2009;6(8):1671-1680. doi:10.5194/bg-6-1671-2009~~

Formatted: Font color: Text 1

Formatted: Font color: Text 1

Formatted: Font: 11 pt, Font color: Text 1

Formatted: Font: 11 pt, Font color: Text 1

Formatted: Font color: Text 1

Formatted: Font color: Text 1

Formatted: Font color: Text 1

Formatted

Formatted: Font color: Text 1

1736 McIlvin, M.R., Casciotti, K.L., 2011. Technical Updates to the Bacterial Method for Nitrate Isotopic Analyses.
1737 Anal. Chem. 83, 1850–1856. <https://doi.org/10.1021/ac1028984>

1738 McMahon, K.W., Williams, B., Guilderson, T.P., Glynn, D.S., McCarthy, M.D., 2018. Calibrating amino acid
1739 $\delta^{13}\text{C}$ and $\delta^{15}\text{N}$ offsets between polyp and protein skeleton to develop proteinaceous deep-sea corals as
1740 paleoceanographic archives. Geochim. Cosmochim. Acta 220, 261–275.
1741 <https://doi.org/10.1016/j.gca.2017.09.048>

1742 Middelburg, J., Mueller, C., Veuger, B. Larsson, A. I., Form, A., van Oevelen, D 2016.. Discovery of symbiotic
1743 nitrogen fixation and chemoautotrophy in cold-water corals. *Sci Rep* 5, 17962 (2016).
1744 <https://doi.org/10.1038/srep17962>

1745 Miller, M., 1995. Growth of a temperate coral: effects of temperature, light, depth, and heterotrophy. Mar. Ecol.
1746 Prog. Ser. 122, 217–225. <https://doi.org/10.3354/meps122217>

1747 Minagawa, M., Wada, E., 1984. Stepwise enrichment of ^{15}N along food chains: Further evidence and the relation
1748 between $\delta^{15}\text{N}$ and animal age. Geochim. Cosmochim. Acta 48, 1135–1140.
1749 [https://doi.org/10.1016/0016-7037\(84\)90204-7](https://doi.org/10.1016/0016-7037(84)90204-7)

1750 ~~Mortensen P.B., (2001) Aquarium observations on the deep-water coral *Lophelia pertusa* (L., 1758) (scleractinia)
1751 and selected associated invertebrates, *Ophelia*, 54:2, 83-104, DOI: 10.1080/00785236.2001.10409457~~

1752 [Muhs, D.R., Kennedy, G.L., Rockwell, T.K., 1994. Uranium-Series Ages of Marine Terrace Corals from the
1753 Pacific Coast of North America and Implications for Last-Interglacial Sea Level History. *Quaternary
1754 Research* 42, 72–87. <https://doi.org/10.1006/qres.1994.1055>](https://doi.org/10.1006/qres.1994.1055)

1755 [Mueller, C.E., Larsson, A.I., Veuger, B., Middelburg, J.J., van Oevelen, D., 2014. Opportunistic feeding on
1756 various organic food sources by the cold-water coral *Lophelia pertusa*. *Biogeosciences* 11, 123–133.
1757 <https://doi.org/10.5194/bg-11-123-2014>](https://doi.org/10.5194/bg-11-123-2014)

1758 [Murray, J.W., Roberts, E., Howard, E., O'Donnell, M., Bantam, C., Carrington, E., Foy, M., Paul, B., Fay, A.,
1759 2015. An inland sea high nitrate-low chlorophyll \(HNLC\) region with naturally high pCO₂. *Limnol.
1760 Oceanogr.* 60, 957–966. <https://doi.org/10.1002/lno.10062>](https://doi.org/10.1002/lno.10062)

1761 Muscatine, L., Goiran, C., Land, L., Jaubert, J., Cuif, J.-P., Allemand, D., 2005. Stable isotopes ($\delta^{13}\text{C}$ and $\delta^{15}\text{N}$)
1762 of organic matrix from coral skeleton. *Proc. Natl. Acad. Sci.* 102, 1525–1530.
1763 <https://doi.org/10.1073/pnas.0408921102>

1764 Naumann, M.S., Orejas, C., Wild, C., Ferrier-Pagès, C., 2011. First evidence for zooplankton feeding sustaining
1765 key physiological processes in a scleractinian cold-water coral. *J. Exp. Biol.* 214, 3570–3576.
1766 <https://doi.org/10.1242/jeb.061390>

1767 Naumann, M.S., Tolosa, I., Taviani, M., Grover, R., Ferrier-Pagès, C., 2015. Trophic ecology of two cold-water
1768 coral species from the Mediterranean Sea revealed by lipid biomarkers and compound-specific isotope
1769 analyses. *Coral Reefs* 34, 1165–1175. <https://doi.org/10.1007/s00338-015-1325-8>

1770 [Pride C, Thunell R, Sigman D, Keigwin L, Altabet M, Tappa E. 1999. Nitrogen isotopic variations in the Gulf of
1771 California since the Last Deglaciation: Response to global climate change. *Paleoceanography* 14\(3\).
1772 doi:10.1029/1999PA900004](https://doi.org/10.1029/1999PA900004)

Formatted: Font color: Text 1

Formatted: Font color: Text 1

~~Mortensen, P.B., Rapp, H.T., Båmstedt, U., 1998. Oxygen and carbon isotope ratios related to growth line patterns in skeletons of *Lophelia pertusa* (L.) (Anthozoa, Scleractinia): Implications for determination of linear extension rate. *Sarsia* 83, 433–446. <https://doi.org/10.1080/00364827.1998.10413702>~~

Formatted: Font color: Text 1

Formatted: Font color: Text 1

Formatted: Font color: Text 1

Formatted: Font color: Text 1

Formatted: Font color: Text 1

Formatted: Font color: Text 1

Formatted: Font color: Text 1

Formatted: Font color: Text 1

Formatted: Font color: Text 1

~~Orejas C, Ferrier-Pagès C, Reynaud S, Tsounis G, Allemand D, Gili JM. 2011. Experimental comparison of skeletal growth rates in the cold water coral *Madrepora oculata* Linnaeus, 1758 and three tropical scleractinian corals. *J Exp Mar Bio Ecol.* 2011;405(1):1–5. doi:<https://doi.org/10.1016/j.jembe.2011.05.008>~~
~~Orejas C, Ferrier-Pagès C, Reynaud S, Gori A and others. 2011. Long-term growth rates of four Mediterranean cold-water coral species maintained in aquaria. *Mar Ecol Prog Ser* 429:57–65. <https://doi.org/10.3354/meps09104>~~
~~Osinga, R., Schutter, M., Griffioen, B. et al. 2011. The Biology and Economics of Coral Growth. *Mar Biotechnol* 13, 658–671 (2011). <https://doi.org/10.1007/s10126-011-9382-7>~~

Formatted: Font color: Text 1

- 1790 Purser A, Larsson AI, Thomsen L, van Oevelen D. 2010. The influence of flow velocity and food concentration
 1791 on *Lophelia pertusa* (Scleractinia) zooplankton capture rates. *J Exp Mar Bio Ecol.* 395(1):55-62.
 1792 doi:<https://doi.org/10.1016/j.jembe.2010.08.013>
- 1793 Rae, J.W.B. 2018. Boron Isotopes in Foraminifera: Systematics, Biomineralisation, and CO₂ Reconstruction. In: ←
 1794 Marschall, H., Foster, G. (eds) Boron Isotopes. Advances in Isotope Geochemistry. Springer, Cham.
 1795 https://doi.org/10.1007/978-3-319-64666-4_5
- 1796 Rangel, M.S., Erler, D., Tagliafico, A., Cowden, K., Scheffers, S., Christidis, L., 2019. Quantifying the transfer
 1797 of prey δ¹⁵N signatures into coral holobiont nitrogen pools. *Mar. Ecol. Prog. Ser.* 610, 33–49.
 1798 <https://doi.org/10.3354/meps12847>.
- 1799 [Ren, H., Sigman, D.M., Meckler, A.N., Plessen, B., Robinson, R.S., Rosenthal, Y., Haug, G.H., 2009.](#)
 1800 [Foraminiferal Isotope Evidence of Reduced Nitrogen Fixation in the Ice Age Atlantic Ocean. *Science*](#)
 1801 [323, 244–248. <https://doi.org/10.1126/science.1165787>](#)
- 1802 Reynaud, S., Martinez, P., Houlbrèque, F., Billy, I., Allemand, D., Ferrier-Pagès, C., 2009. Effect of light and
 1803 feeding on the nitrogen isotopic composition of a zooxanthellate coral: role of nitrogen recycling. *Mar.*
 1804 *Ecol. Prog. Ser.* 392, 103–110. <https://doi.org/10.3354/meps08195>
- 1805 Roberts, J.M., Wheeler, A.J., Freiwald, A., 2006. Reefs of the deep: The biology and geology of cold-water coral
 1806 ecosystems. *Science* 312, 543–547. <https://doi.org/10.1126/science.1119861>
- 1807 Robinson, R.S., Kienast, M., Albuquerque, A.L., Altabet, M., Contreras, S., Holz, R.D.P., Dubois, N., Francois,
 1808 R., Galbraith, E., Hsu, T.-C., Ivanochko, T., Jaccard, S., Kao, S.-J., Kiefer, T., Kienast, S., Lehmann, M.,
 1809 Martinez, P., McCarthy, M., Möbius, J., Pedersen, T., Quan, T.M., Ryabenko, E., Schmittner, A.,
 1810 Schneider, R., Schneider-Mor, A., Shigemitsu, M., Sinclair, D., Somes, C., Studer, A., Thunell, R., Yang,
 1811 J.-Y., 2012. A review of nitrogen isotopic alteration in marine sediments. *Paleoceanography* 27.
 1812 <https://doi.org/10.1029/2012PA002321>
- 1813 Robinson LF, Adkins JF, Frank N, Gagnon, A.C., Prouty, N.G., Roark, B. van de Fliedert, T. 2014. The
 1814 geochemistry of deep-sea coral skeletons: A review of vital effects and applications for
 1815 palaeoceanography. *Deep Sea Res Part II Top Stud Oceanogr.* 99:184-198.
 1816 doi:<https://doi.org/10.1016/j.dsr2.2013.06.005>
- 1817 Robinson RS, Sigman DM. 2008. Nitrogen isotopic evidence for a poleward decrease in surface nitrate within the
 1818 ice age Antarctic. *Quat Sci Rev.* 27(9-10). doi:10.1016/j.quascirev.2008.02.005
- 1819 Robinson, R.S., Smart, S.M., Cybulski, J.D., McMahon, K.W., Marcks, B., Nowakowski, C., 2023. Insights from
 1820 fossil-bound nitrogen isotopes in diatoms, foraminifera, and corals. *Annu. Rev. Mar. Sci.* 15, null.
 1821 <https://doi.org/10.1146/annurev-marine-032122-104001>
- 1822 [Ryan, W. B. F., S.M. Carbotte, J. Coplan, S. O'Hara, A. Melkonian, R. Arko, R.A. Weissel, V. Ferrini, A.](#)
 1823 [Goodwillie, F. Nitsche, J. Bonczkowski, R. Zemsky, 2009, Global Multi-Resolution Topography](#)
 1824 [\(GMRT\) synthesis data set, *Geochem. Geophys. Geosyst.*, 10, Q03014, doi:10.1029/2008GC002332](#)
- 1825 Saino, T., Hattori, A., 1987. Geographical variation of the water column distribution of suspended particulate
 1826 organic nitrogen and its ¹⁵N natural abundance in the Pacific and its marginal seas. *Deep Sea Res. A* 34,
 1827 807–827. [https://doi.org/10.1016/0198-0149\(87\)90038-0](https://doi.org/10.1016/0198-0149(87)90038-0)

Formatted: Normal, Indent: Left: 0", Hanging: 0.5", Space Before: 0 pt, After: 0 pt

Deleted: ¶

Formatted: Font: 12 pt, Font color: Auto

Formatted: Font color: Text 1

Deleted: ¶

Formatted: Hyperlink, Font color: Auto

Formatted: Font: 12 pt, Font color: Auto

Field Code Changed

Deleted: Ren,

Deleted: H., Chen, Y.-C., Wang, X.T., Wong, G.T.F., Cohen, A.L., DeCarlo, T.M., Weigand, M.A., Mii, H.-S., Sigman, D.M., 2017. 21st-century rise in anthropogenic nitrogen deposition on a remote coral reef. *Science* 356, 749–752.

Formatted: Font: Font color: Auto

Formatted: Font: 11 pt

Formatted: Font: 11 pt

Formatted: Font: Font color: Auto

Formatted: Font color: Text 1

Formatted: Font color: Text 1

Formatted: Font color: Text 1

Formatted: Hyperlink, Font color: Auto

Field Code Changed

Formatted: Font: (Default) +Body (Times New Roman), 11 pt

Formatted: Font: (Default) +Body (Times New Roman), 11 pt

Formatted: Font: (Default) +Body (Times New Roman), 11 pt

Formatted: Font: (Default) +Body (Times New Roman), 11 pt

Formatted: Font: (Default) +Body (Times New Roman), 11 pt

Formatted: Font color: Text 1

- 1835 Scrimgeour, C.M., Gordon, S.C., Handley, L.L., Woodford, J.A.T., 1995. Trophic levels and anomalous $\delta^{15}\text{N}$ of
 1836 insects on raspberry (*Rubus Idaeus* L.). *Isotopes Environ. Health Stud.* 31, 107–115.
 1837 <https://doi.org/10.1080/10256019508036256>
- 1838 Sebens, K.P., Vandersall, K.S., Savina, L.A., Graham, K.R., 1996. Zooplankton capture by two scleractinian
 1839 corals, *Madracis mirabilis* and *Montastrea cavernosa*, in a field enclosure. *Mar. Biol.* 127, 303–317.
 1840 <https://doi.org/10.1007/BF00942116>
- 1841 Sherwood, O.A., Heikoop, J.M., Scott, D.B., Risk, M.J., Guilderson, T.P., McKinney, R.A., 2005. Stable isotopic
 1842 composition of deep-sea gorgonian corals *Primnoa* spp.: a new archive of surface processes. *Mar. Ecol.*
 1843 *Prog. Ser.* 301, 135–148. <https://doi.org/10.3354/meps301135>
- 1844 Sherwood, O.A., Jamieson, R.E., Edinger, E.N., Wareham, V.E., 2008. Stable C and N isotopic composition of
 1845 cold-water corals from the Newfoundland and Labrador continental slope: Examination of trophic, depth
 1846 and spatial effects. *Deep Sea Res. Part Oceanogr. Res. Pap.* 55, 1392–1402.
 1847 <https://doi.org/10.1016/j.dsr.2008.05.013>
- 1848 Sherwood, O.A., Thresher, R.E., Fallon, S.J., Davies, D.M., Trull, T.W., 2009. Multi-century time-series of ^{15}N
 1849 and ^{14}C in bamboo corals from deep Tasmanian seamounts: evidence for stable oceanographic
 1850 conditions. *Mar. Ecol. Prog. Ser.* 397, 209–218. <https://doi.org/10.3354/meps08166>
- 1851 Sigman, D.M., Altabet, M.A., McCorkle, D.C., Francois, R., Fischer, G., 1999. The $\delta^{15}\text{N}$ of nitrate in the
 1852 Southern Ocean: Consumption of nitrate in surface waters. *Glob. Biogeochem. Cycles* 13, 1149–1166.
 1853 <https://doi.org/10.1029/1999GB900038>
- 1854 Sigman, D., Boyle, E. Glacial/interglacial variations in atmospheric carbon dioxide. 2000. *Nature* 407, 859–869
 1855 (2000). <https://doi.org/10.1038/35038000>
- 1856 Sigman, D.M., Casciotti, K.L., Andreani, M., Barford, C., Galanter, M., Böhlke, J.K., 2001. A Bacterial method
 1857 for the nitrogen isotopic analysis of nitrate in seawater and freshwater. *Anal. Chem.* 73, 4145–4153.
 1858 <https://doi.org/10.1021/ac010088e>
- 1859 Sigman, D.M., Fripiat, F., 2019. *Nitrogen Isotopes in the Ocean*, in: Cochran, J.K., Bokuniewicz, H.J., Yager,
 1860 P.L. (Eds.), *Encyclopedia of Ocean Sciences (Third Edition)*. Academic Press, Oxford, pp. 263–278.
 1861 <https://doi.org/10.1016/B978-0-12-409548-9.11605-7>
- 1862 Soetaert, K., Mohn, C., Rengstorf, A., Grehan, A., van Oevelen, D., 2016. Ecosystem engineering creates a direct
 1863 nutritional link between 600-m deep cold-water coral mounds and surface productivity. *Sci. Rep.* 6,
 1864 35057. <https://doi.org/10.1038/srep35057>
- 1865 Spero, H.J., Andreasen, D.J., Sorgeloos, P., 1993. Carbon and nitrogen isotopic composition of different strains
 1866 of *Artemia* sp. *Int. J. Salt Lake Res.* 2, 133. <https://doi.org/10.1007/BF02905905>
- 1867 Studer, A.S., Sigman, D.M., Martinez-Garcia, A., Thole, L.M., Michel, E., Jaccard, S.L., Lippolds, J.A., Mazaud,
 1868 A., Wang, X.C.T., Robinson, L.F., Adkins, J.F., Haug, G.H., 2018. Increased nutrient supply to the
 1869 Southern Ocean during the Holocene and its implications for the pre-industrial atmospheric CO₂ rise.
 1870 *Nat Geosci* 11, 756–761
- 1871 Tanaka, Y., Miyajima, T., Koike, I., Hayashibara, T., Ogawa, H., 2006. Translocation and conservation of
 1872 organic nitrogen within the coral-zooxanthella symbiotic system of *Acropora pulchra*, as demonstrated

Formatted: Font color: Text 1

Formatted: Font color: Text 1

Deleted: Schutter, M., Crocker, J., Pajmans, A., Janse, M., Ozinga, R., Verreth, J.A.J., Wijffels, R.H. 2010. The effect of different flow regimes on the growth and metabolic rates of the scleractinian coral *Galaxea fascicularis*. *Coral Reefs* 29, 737–748. <https://doi.org/10.1007/s00338-010-0617-2>

Formatted: Font color: Text 1

Formatted: Font color: Text 1

Formatted: Font color: Text 1

Formatted: Font color: Text 1

Formatted: Font color: Text 1

Formatted: Font color: Text 1

Formatted: Font color: Text 1

Formatted: Hyperlink, Font: 12 pt, Font color: Auto

Field Code Changed

Formatted: Font: 11 pt

Formatted: Indent: Left: 0", Hanging: 0.5"

Deleted: ¶

Formatted: Font color: Text 1

- 1879 by dual isotope-labeling techniques. *J. Exp. Mar. Biol. Ecol.* 336, 110–119.
 1880 <https://doi.org/10.1016/j.jembe.2006.04.011>
- 1881 Tanaka, Y., Suzuki, A., Sakai, K., 2018. The stoichiometry of coral-dinoflagellate symbiosis: carbon and nitrogen
 1882 cycles are balanced in the recycling and double translocation system. *ISME J.* 12, 860–868.
 1883 <https://doi.org/10.1038/s41396-017-0019-3>
- 1884 Teece, M.A., Estes, B., Gelsleichter, E., Lirman, D., 2011. Heterotrophic and autotrophic assimilation of fatty
 1885 acids by two scleractinian corals, *Montastraea faveolata* and *Porites astreoides*. *Limnol. Oceanogr.* 56,
 1886 1285–1296. <https://doi.org/10.4319/lo.2011.56.4.1285>
- 1887 Thiagarajan N., Subhas A. V., Southon J. R., Eiler J. M. and Adkins J. F. 2014. Abrupt pre-Bolling-Allerod
 1888 warming and circulation changes in the deep ocean. *Nature* 511, 75–78.
 1889 <https://doi.org/10.1038/nature13472>
- 1890 Thiem, Ø., Ravagnan, E., Fosså, J.H., Berntsen, J., 2006. Food supply mechanisms for cold-water corals along a
 1891 continental shelf edge. *J. Mar. Syst.* 60, 207–219. <https://doi.org/10.1016/j.jmarsys.2005.12.004>
- 1892 Thomas, S.M., Crowther, T.W., 2015. Predicting rates of isotopic turnover across the animal kingdom: a
 1893 synthesis of existing data. *J. Anim. Ecol.* 84, 861–870. <https://doi.org/10.1111/1365-2656.12326>
- 1894 ~~Treibergs, L.A., Fawcett, S.E., Lomas, M.W., Sigman, D.M., 2014. Nitrogen isotopic response of prokaryotic and
 1895 eukaryotic phytoplankton to nitrate availability in Sargasso Sea surface waters. *Limnol. Oceanogr.* 59,
 1896 972–985. <https://doi.org/10.4319/lo.2014.59.3.0972>~~
- 1897 Tsounis G, Orejas C, Reynaud S, JM G, Allemand D, Ferrier-Pagès C. 2010. Prey-capture rates in four
 1898 Mediterranean cold water corals. *Mar Ecol Prog Ser.* 398:149-155. <https://doi.org/10.3354/meps08312>
- 1899 van Oevelen, P., Duineveld, G., Lavaleye, M., Mienis, Furu, Soetaert, Karlina, H., Carlo H. R., 2009. The cold-
 1900 water coral community as hotspot of carbon cycling on continental margins: A food-web analysis from
 1901 Rockall Bank (northeast Atlantic), *Limnology and Oceanography*, 54, doi: 10.4319/lo.2009.54.6.1829
- 1902 ~~Vinogradov, M. E. Feeding of the deep-sea zooplankton. 1962. *Rapp. Pv. Reun. Cons. Perm. Int. Exp. Mer.* 153,
 1903 114–120.~~
- 1904 Wang, X.T., Prokopenko, M.G., Sigman, D.M., Adkins, J.F., Robinson, L.F., Ren, H., Oleynik, S., Williams, B.,
 1905 Haug, G.H., 2014. Isotopic composition of carbonate-bound organic nitrogen in deep-sea scleractinian
 1906 corals: A new window into past biogeochemical change. *Earth Planet. Sci. Lett.* 400, 243–250.
 1907 <https://doi.org/10.1016/j.epsl.2014.05.048>
- 1908 Wang, X.T., Sigman, D.M., Prokopenko, M.G., Adkins, J.F., Robinson, L.F., Hines, S.K., Chai, J., Studer, A.S.,
 1909 Martínez-García, A., Chen, T., Haug, G.H., 2017. Deep-sea coral evidence for lower Southern Ocean
 1910 surface nitrate concentrations during the last ice age. *Proc. Natl. Acad. Sci.* 114, 3352–3357.
 1911 <https://doi.org/10.1073/pnas.1615718114>
- 1912 Webb, S., Hedges, R., Simpson, S., 1998. Diet quality influences the $\delta^{13}\text{C}$ and $\delta^{15}\text{N}$ of locusts and their
 1913 biochemical components. *J. Exp. Biol.* 201, 2903–2911. <https://doi.org/10.1242/jeb.201.20.2903>
- 1914 Weigand, M.A., Foriel, J., Barnett, B., Oleynik, S., Sigman, D.M., 2016. Updates to instrumentation and
 1915 protocols for isotopic analysis of nitrate by the denitrifier method. *Rapid Commun. Mass Spectrom.* 30,
 1916 1365–1383. <https://doi.org/10.1002/rcm.7570>

Formatted: Font color: Text 1

Formatted: Font color: Text 1

Formatted: No underline, Font color: Text 1

Formatted: Font color: Text 1

Formatted: Font color: Text 1

Formatted: Font color: Text 1

Deleted: ¶

Formatted: Font color: Text 1, Strikethrough

Formatted: Font color: Text 1

Formatted: Font color: Text 1

Formatted: Font color: Text 1

1918 Williams, B., and Grottole, A. G. 2010. Recent shoaling of the nutricline and thermocline in the western tropical
1919 Pacific, *Geophys. Res. Lett.*, 37, L22601, doi:10.1029/2010GL044867.

1920 Zhang, R., X. T. Wang, H. Ren, J. Huang, M. Chen, and D. M. Sigman. 2020. Dissolved Organic Nitrogen
1921 Cycling in the South China Sea From an Isotopic Perspective. *Glob. Biogeochem. Cycles* 34:
1922 e2020GB006551. doi:10.1029/2020GB006551.

1923 Zhou, M., Granger, J., Chang, B.X., 2022. Influence of sample volume on nitrate N and O isotope ratio analyses
1924 with the denitrifier method. *Rapid Commun. Mass Spectrom.* 36, e9224.
1925 <https://doi.org/10.1002/rcm.9224>

Formatted: Font color: Text 1

Formatted: Font color: Text 1

Formatted: Font color: Text 1

Formatted: Font color: Text 1

~~Deleted: Wishner, K.F., Meise-Munns, C.J., 1984. In situ grazing rates of deep-sea benthic boundary layer zooplankton. *Mar. Biol.* 84, 65–74. <https://doi.org/10.1007/BF00394528>~~

Formatted: Font color: Text 1

Page 1: [1] Formatted Anne M Gothmann 12/6/23 7:59:00 AM

Font: 16 pt, Font color: Text 1

Page 1: [1] Formatted Anne M Gothmann 12/6/23 7:59:00 AM

Font: 16 pt, Font color: Text 1

Page 1: [2] Formatted Anne M Gothmann 12/6/23 7:59:00 AM

Font color: Text 1

Page 1: [2] Formatted Anne M Gothmann 12/6/23 7:59:00 AM

Font color: Text 1

Page 1: [3] Formatted Anne M Gothmann 11/14/23 3:33:00 PM

Font: 12 pt

Page 1: [3] Formatted Anne M Gothmann 11/14/23 3:33:00 PM

Font: 12 pt

Page 1: [4] Deleted Masha Prokopenko 11/20/23 1:50:00 PM

Page 1: [4] Deleted Masha Prokopenko 11/20/23 1:50:00 PM

Page 1: [4] Deleted Masha Prokopenko 11/20/23 1:50:00 PM

Page 1: [5] Formatted Anne M Gothmann 11/14/23 3:33:00 PM

Font: 12 pt, Font color: Auto

Page 1: [5] Formatted Anne M Gothmann 11/14/23 3:33:00 PM

Font: 12 pt, Font color: Auto

Page 1: [6] Deleted Anne M Gothmann 12/6/23 8:09:00 AM

Page 1: [6] Deleted Anne M Gothmann 12/6/23 8:09:00 AM

Page 1: [7] Formatted Anne M Gothmann 11/14/23 3:33:00 PM

Font: 12 pt, Font color: Auto

Page 1: [7] Formatted Anne M Gothmann 11/14/23 3:33:00 PM

Font: 12 pt, Font color: Auto

Page 1: [8] Deleted Anne M Gothmann 12/6/23 8:10:00 AM

Page 1: [8] Deleted Anne M Gothmann 12/6/23 8:10:00 AM

Page 1: [9] Formatted Anne M Gothmann 11/14/23 3:33:00 PM

Font: 12 pt

Page 1: [9] Formatted Anne M Gothmann 11/14/23 3:33:00 PM

Font: 12 pt

Page 1: [10] Formatted Anne M Gothmann 11/14/23 3:33:00 PM

Font: 12 pt, Font color: Auto

▲ **Page 1: [10] Formatted** Anne M Gothmann 11/14/23 3:33:00 PM

Font: 12 pt, Font color: Auto

▲ **Page 1: [11] Deleted** Anne M Gothmann 12/6/23 8:11:00 AM

▼ **Page 1: [11] Deleted** Anne M Gothmann 12/6/23 8:11:00 AM

▼ **Page 1: [11] Deleted** Anne M Gothmann 12/6/23 8:11:00 AM

▼ **Page 1: [12] Deleted** Masha Prokopenko 11/20/23 2:39:00 PM

▲ **Page 13: [13] Formatted** Anne M Gothmann 11/14/23 3:33:00 PM

Font color: Text 1

▲ **Page 13: [13] Formatted** Anne M Gothmann 11/14/23 3:33:00 PM

Font color: Text 1

▲ **Page 13: [13] Formatted** Anne M Gothmann 11/14/23 3:33:00 PM

Font color: Text 1

▲ **Page 13: [13] Formatted** Anne M Gothmann 11/14/23 3:33:00 PM

Font color: Text 1

▲ **Page 13: [13] Formatted** Anne M Gothmann 11/14/23 3:33:00 PM

Font color: Text 1

▲ **Page 13: [13] Formatted** Anne M Gothmann 11/14/23 3:33:00 PM

Font color: Text 1

▲ **Page 13: [13] Formatted** Anne M Gothmann 11/14/23 3:33:00 PM

Font color: Text 1

▲ **Page 13: [13] Formatted** Anne M Gothmann 11/14/23 3:33:00 PM

Font color: Text 1

▲ **Page 13: [13] Formatted** Anne M Gothmann 11/14/23 3:33:00 PM

Font color: Text 1

▲ **Page 13: [13] Formatted** Anne M Gothmann 11/14/23 3:33:00 PM

Font color: Text 1

▲ **Page 13: [13] Formatted** Anne M Gothmann 11/14/23 3:33:00 PM

Font color: Text 1

▲ **Page 13: [13] Formatted** Anne M Gothmann 11/14/23 3:33:00 PM

Font color: Text 1

▲ **Page 13: [13] Formatted** Anne M Gothmann 11/14/23 3:33:00 PM

Font color: Text 1

▲ **Page 13: [13] Formatted** Anne M Gothmann 11/14/23 3:33:00 PM

Font color: Text 1

▲ **Page 13: [13] Formatted** Anne M Gothmann 11/14/23 3:33:00 PM

Font color: Text 1

▲ **Page 13: [13] Formatted** Anne M Gothmann 11/14/23 3:33:00 PM

Font color: Text 1

▲ **Page 13: [13] Formatted** Anne M Gothmann 11/14/23 3:33:00 PM

Font color: Text 1

▲ **Page 13: [13] Formatted** Anne M Gothmann 11/14/23 3:33:00 PM

Font color: Text 1

▲ **Page 13: [13] Formatted** Anne M Gothmann 11/14/23 3:33:00 PM

Font color: Text 1

▲ **Page 13: [13] Formatted** Anne M Gothmann 11/14/23 3:33:00 PM

Font color: Text 1

▲ **Page 13: [13] Formatted** Anne M Gothmann 11/14/23 3:33:00 PM

Font color: Text 1

▲ **Page 13: [13] Formatted** Anne M Gothmann 11/14/23 3:33:00 PM

Font color: Text 1

▲ **Page 13: [13] Formatted** Anne M Gothmann 11/14/23 3:33:00 PM

Font color: Text 1

▲ **Page 13: [13] Formatted** Anne M Gothmann 11/14/23 3:33:00 PM

Font color: Text 1

▲ **Page 13: [14] Formatted** Anne M Gothmann 11/14/23 3:33:00 PM

Font color: Text 1

▲ **Page 13: [14] Formatted** Anne M Gothmann 11/14/23 3:33:00 PM

Font color: Text 1

▲ **Page 13: [14] Formatted** Anne M Gothmann 11/14/23 3:33:00 PM

Font color: Text 1

▲ **Page 13: [14] Formatted** Anne M Gothmann 11/14/23 3:33:00 PM

Font color: Text 1

▲ **Page 13: [14] Formatted** Anne M Gothmann 11/14/23 3:33:00 PM

Font color: Text 1

▲ **Page 13: [14] Formatted** Anne M Gothmann 11/14/23 3:33:00 PM

Font color: Text 1

▲ **Page 13: [15] Deleted** Julie Granger 10/31/23 11:20:00 AM

x.....▲.....←

Page 13: [15] Deleted Julie Granger 10/31/23 11:20:00 AM

x.....▲.....←

Page 13: [16] Deleted Anne M Gothmann 10/17/23 7:56:00 AM

x.....▲.....←

Page 13: [16] Deleted Anne M Gothmann 10/17/23 7:56:00 AM

Page 13: [16] Deleted Anne M Gothmann 10/17/23 7:56:00 AM

Page 13: [16] Deleted Anne M Gothmann 10/17/23 7:56:00 AM

Page 24: [17] Formatted Anne M Gothmann 11/14/23 3:51:00 PM

Indent: First line: 0.25", Space After: 0 pt, Line spacing: 1.5 lines, Don't adjust space between Latin and Asian text, Don't adjust space between Asian text and numbers

Page 24: [18] Deleted Anne M Gothmann 11/14/23 3:44:00 PM

Page 26: [19] Deleted Anne M Gothmann 11/14/23 3:49:00 PM

Page 28: [20] Deleted Anne M Gothmann 10/25/23 10:58:00 AM

Page 28: [20] Deleted Anne M Gothmann 10/25/23 10:58:00 AM

Page 28: [20] Deleted Anne M Gothmann 10/25/23 10:58:00 AM

Page 28: [20] Deleted Anne M Gothmann 10/25/23 10:58:00 AM

Page 28: [20] Deleted Anne M Gothmann 10/25/23 10:58:00 AM

Page 28: [21] Deleted Masha Prokopenko 10/31/23 11:38:00 PM

Page 28: [21] Deleted Masha Prokopenko 10/31/23 11:38:00 PM

Page 28: [22] Formatted Anne M Gothmann 11/14/23 3:33:00 PM

Font color: Text 1

▲ **Page 28: [22] Formatted Anne M Gothmann 11/14/23 3:33:00 PM**

Font color: Text 1

▲ **Page 28: [22] Formatted Anne M Gothmann 11/14/23 3:33:00 PM**

Font color: Text 1

▲ **Page 28: [22] Formatted Anne M Gothmann 11/14/23 3:33:00 PM**

Font color: Text 1

▲ **Page 28: [23] Deleted Masha Prokopenko 10/31/23 11:32:00 PM**

x

▲ **Page 28: [23] Deleted Masha Prokopenko 10/31/23 11:32:00 PM**

x

▲ **Page 28: [24] Formatted Anne M Gothmann 11/14/23 3:33:00 PM**

Font: Italic, Font color: Text 1

▲ **Page 28: [24] Formatted Anne M Gothmann 11/14/23 3:33:00 PM**

Font: Italic, Font color: Text 1

▲ **Page 28: [25] Deleted Anne M Gothmann 11/14/23 8:20:00 PM**

x

▲ **Page 28: [26] Deleted Masha Prokopenko 11/24/23 6:40:00 AM**

v

▲ **Page 28: [26] Deleted Masha Prokopenko 11/24/23 6:40:00 AM**

v

▲ **Page 28: [27] Formatted Anne M Gothmann 11/14/23 3:33:00 PM**

Font color: Text 1

▲ **Page 28: [27] Formatted Anne M Gothmann 11/14/23 3:33:00 PM**

Font color: Text 1

▲ **Page 28: [28] Deleted Anne M Gothmann 11/14/23 8:18:00 PM**

x

▲ **Page 28: [29] Deleted Masha Prokopenko 11/1/23 12:18:00 AM**

x

▲ **Page 28: [29] Deleted Masha Prokopenko 11/1/23 12:18:00 AM**

x

Page 28: [29] Deleted Masha Prokopenko 11/1/23 12:18:00 AM

x.....<
▲.....

Page 29: [30] Deleted Masha Prokopenko 11/25/23 1:13:00 PM

x.....<
▲.....

Page 29: [30] Deleted Masha Prokopenko 11/25/23 1:13:00 PM

x.....<
▲.....

Page 29: [31] Deleted Anne M Gothmann 10/16/23 12:21:00 PM

x.....<
▲.....

Page 29: [31] Deleted Anne M Gothmann 10/16/23 12:21:00 PM

x.....<
▲.....

Page 29: [31] Deleted Anne M Gothmann 10/16/23 12:21:00 PM

x.....<
▲.....

Page 29: [32] Deleted Masha Prokopenko 11/1/23 12:23:00 AM

x.....<
▲.....

Page 29: [32] Deleted Masha Prokopenko 11/1/23 12:23:00 AM

x.....<
▲.....

Page 29: [33] Deleted Masha Prokopenko 11/1/23 12:26:00 AM

x.....<
▲.....

Page 29: [33] Deleted Masha Prokopenko 11/1/23 12:26:00 AM

x.....<
▲.....

Page 29: [33] Deleted Masha Prokopenko 11/1/23 12:26:00 AM

x.....<
▲.....

Page 29: [33] Deleted Masha Prokopenko 11/1/23 12:26:00 AM

x.....<
▲.....

Page 29: [33] Deleted Masha Prokopenko 11/1/23 12:26:00 AM

x.....<
▲.....

Page 29: [34] Deleted Anne M Gothmann 10/17/23 8:34:00 AM

Page 29: [34] Deleted Anne M Gothmann 10/17/23 8:34:00 AM

Page 29: [35] Deleted Anne M Gothmann 10/15/23 9:05:00 AM

Page 29: [35] Deleted Anne M Gothmann 10/15/23 9:05:00 AM

Page 29: [35] Deleted Anne M Gothmann 10/15/23 9:05:00 AM

Page 29: [35] Deleted Anne M Gothmann 10/15/23 9:05:00 AM

Page 29: [35] Deleted Anne M Gothmann 10/15/23 9:05:00 AM

Page 29: [35] Deleted Anne M Gothmann 10/15/23 9:05:00 AM

Page 29: [35] Deleted Anne M Gothmann 10/15/23 9:05:00 AM

Page 29: [35] Deleted Anne M Gothmann 10/15/23 9:05:00 AM

Page 29: [36] Formatted Anne M Gothmann 11/14/23 3:33:00 PM

Font color: Text 1

Page 29: [36] Formatted Anne M Gothmann 11/14/23 3:33:00 PM

Font color: Text 1

Page 29: [37] Formatted Anne M Gothmann 11/14/23 3:33:00 PM

Font color: Text 1

Page 29: [37] Formatted Anne M Gothmann 11/14/23 3:33:00 PM

Font color: Text 1

Page 29: [38] Deleted Masha Prokopenko 11/1/23 12:29:00 AM

Page 33: [39] Formatted Anne M Gothmann 11/14/23 3:33:00 PM

Font: (Default) +Headings (Times New Roman), No underline, Font color: Text 1

Font: (Default) +Headings (Times New Roman), 12 pt, Font color: Text 1